17432

NAME OF AUTHOR...... Juan Anhi ....

TITLE OF THESIS.....A.n...Investigation Into The
Functional Relationship Between
The Capillary Pressure And
Saturation In Porous Medium

UNIVERSITY.....Ø...Univ....of...Alberta.............

DEGREE FOR WHICH THESIS WAS PRESENTED.......M. Sc............

YEAR THIS DEGREE GRANTED......1973...................

(Signed).....Juan Anhi.....

PERMANENT ADDRESS:

#.609...12021.....

.....Jasper Ave...

Edmonton, Alta.

DATED /August...28...19 73.

NL-91 (10-68)

THE UNIVERSITY OF ALBERTA

AN INVESTIGATION INTO THE FUNCTIONAL RELATIONSHIP BETWEEN

THE CAPILLARY PRESSURE AND SATURATION IN POROUS MEDIA

by

Ⓒ Jun Anli

A THESIS

SUBMITTED TO THE FACULTY OF GRADUATE STUDIES AND RESEARCH

IN PARTIAL FULFILMENT OF THE REQUIREMENTS FOR THE DEGREE

OF MASTER OF SCIENCE IN PETROLEUM ENGINEERING

DEPARTMENT OF MINERAL ENGINEERING

EDMONTON, ALBERTA

FALL, 1973

THE UNIVERSITY OF ALBERTA

FACULTY OF GRADUATE STUDIES AND RESEARCH

The undersigned certify that they have read, and
recommend to the Faculty of Graduate Studies and Research
for acceptance, a thesis entitled "An Investigation into
the Functional Relationship between the Capillary Pressure
and Saturation in Porous Media" submitted by Jun Anli in
partial fulfilment of the requirements for the degree of
Master of Science in Petroleum Engineering.

....
Supervisor

Date *August 24, 1973*

ABSTRACT

The modeling of physical phenomena is a useful tool for scientists and engineers in representing the important characteristics of the actual mechanism. A capillary pressure function for porous media (commonly known as the J-function) was given by Leverett and has been widely used in Petroleum Engineering. However, his model is known to correlate satisfactorily only the data from unconsolidated sands and from the same formation. It is the purpose of this study to formulate a new drainage capillary pressure function in an attempt to eliminate this restriction.

The new model suggested here is a function of saturation and involves three parameters which have to be obtained experimentally. Results obtained from the centrifuge method together with literature data were used to test this model.

The model satisfactorily correlates literature data regardless of the wetting-non-wetting fluid combinations. A capillary pressure curve generated from centrifuge data, using this model, agrees well with that obtained using a modified Hassler method. These results indicate that the model is satisfactory and that it may be regarded as universal.

iv

ACKNOWLEDGEMENTS

The author expresses his thanks to Dr. R. G. Bentsen
for his advice and understanding in the supervision of this
project.

Special thanks are due to the personnel of the
Chemical and Petroleum Engineering machine and instrument
shops without whom the construction of the equipment would
not have been possible.

Thanks are due to many individuals of the Department
of Chemical and Petroleum Engineering for their helpful
suggestions.

To the author's family for their encouragement during
this study, the author expresses his gratitude.

Special acknowledgements are made to the National
Research Council of Canada and the Faculty of Engineering
Petroleum Education Plan B for the necessary funds for this
study.

TABLE OF CONTENTS

LIST OF TABLES

LIST OF FIGURES

x

CHAPTER I

INTRODUCTION

In petroleum reservoirs two fluids exist, and often three fluid phases are present. The co-existence of two or more phases in a porous medium gives rise to capillary forces.

Although the absolute magnitude of the capillary pressure in most petroleum reservoirs is not large, the effects of capillary forces are extremely important in petroleum production. Firstly, the original distribution of fluids in the reservoir rock is controlled by gravitational and capillary forces.[34,35] Secondly, during the production process, the relative freedom of movement and the distribution of fluids are primarily influenced by these forces. And finally, capillary forces are responsible for trapping a large portion of the non-wetting fluid within the interstices of the rock. For these reasons the understanding of capillary forces is essential in petroleum production.

It is of interest, therefore, to develop an equation which describes capillary effects in porous media. It is also of interest to express such an equation in a universal form so that any capillary pressure curve could be reduced to a single curve.

Leverett[28] gave the essential concepts of the capillary pressure in a porous medium. He defined the term "capillary pressure" and proposed a universal capillary

pressure function, commonly called the J-function, which correlates the physical properties of a porous medium and fluids and the capillary pressure. It has been noted, however, that the J-function is not truly satisfactory when data are taken from rock samples with various lithologic properties rather than from samples of similar lithologic type. A possible explanation to this problem may be that the J-function does not consider the wetting properties of the medium.

It is the purpose of this study to devise a universal function for drainage capillary pressure-fluid saturation relationship. One of the parameters involved in the proposed capillary pressure model incorporates the effects of interfacial tension, wettability and pore-size distribution. It is thus possible to reduce capillary pressure curves taken from various rock samples to a single curve.

A technique for using the model with data obtained in a centrifuge is presented. The results obtained using the proposed model agree well with the results obtained using Hassler's[19] technique.

CHAPTER II

THEORY AND LITERATURE REVIEW

A. Surface Free Energy, Surface Tension and Interfacial Tension

At the boundary of various phases in the reservoir exist the forces resulting from the molecular action between the phases. The physical forces of molecular attraction, generally known as van der Waals forces, are the fundamental basis for explaining various boundary phenomena. The van der Waals forces between two molecules are proportional to the product of their masses and inversely proportional to the square of the distance between them.

A molecule in the bulk fluid is surrounded completely by other molecules; thus it is attracted evenly to all directions. However, a molecule at the boundary of any two phases, i.e. gas and liquid, liquid and liquid, or liquid and solid, is surrounded by the molecules of the other phase also, thus the net forces acting on the molecule result in unbalanced attraction. As a result, the boundary surface tends to contract to a minimum possible area. This spontaneous contraction of the surface indicates that free energy is involved.

In order to create a unit area of new boundary,

work comparable to the number of molecules in the unit area is required. It may also be said that a certain amount of work is required to bring a molecule from the bulk of a fluid into the interface against the unbalanced molecular forces. The amount of work necessary, in ergs, to move molecules into the boundary to create a unit area of new surface is referred to as "the surface free energy" of the substance.[10]

The term "surface tension" is more frequently used as the boundary surface tends to contract and behaves as if it were in a state of tension. However, the surface tension is really a measure of the surface free energy. It is defined as the force in dynes acting along the boundary surface of the fluid perpendicular to any 1 cm in length. Thus the surface tension is equal, both numerically and dimensionally, to the surface free energy. When the two phases are both liquid, the term "interfacial tension" is used.

B. Wetting

Where two immiscible liquids or a liquid and a solid are in phase contact, the surface molecules of each substance are attracted across the interface by van der Waals forces. This attraction which is called the "energy of adhesion" or "adhesion tension", differs from interfacial tension, which is a property of the interface and is the differential resultant pull away from it.[29]

For an oil-water-rock system, such as a reservoir, adhesion tension is defined as follows:

$$A_t = \gamma_{so} - \gamma_{sw} = \gamma_{wo} \cos \theta \qquad (II - 1)$$

or

$$\cos \theta = \frac{\gamma_{so} - \gamma_{sw}}{\gamma_{wo}} \qquad (II - 2)$$

The adhesion tension, or the magnitude of the contact angle, is the measure of the wetting properties of the solid by the fluids. Equation II-2 states that if adhesion tension is zero, that is to say, if θ is 90°, the interfacial tension $\gamma_{so} = \gamma_{sw}$. This indicates that the oil and the water have equal affinity to the solid surface. If, however, $\gamma_{so} > \gamma_{sw}$, $\cos \theta$ would be positive and the contact angle would have a value between 90° and zero; then water would preferentially wet the solid surface. Conversely, if $\gamma_{so} < \gamma_{sw}$, θ would have the angle between 90° and 180°; thus oil would wet the solid surface. In short, the magnitude of the interfacial contact angle serves as a definite criterion for the wetting of the solid by the fluids involved.[4]

Contact angle of a solid has been measured directly by various workers.[4,23,50] A smooth surface is necessary in this measurement. Most solid surfaces, however, do not have

perfect smoothness. Wenzel[52] introduced a roughness factor to correlate the actual contact angle to the observed angle:

$$\cos \theta' = r \cos \theta \qquad\qquad (II - 3)$$

where

θ' : measured contact angle

θ : actual contact angle

r : roughness factor = actual surface/ geometric surface

However, the direct measurement of contact angle of a porous medium is not practical as the surface is normally extremely rough due to the occurance of pores. Various authors have reported that contact angle of a porous medium can be calculated from the displacement[1,3,45] and the imbibition[5,17] properties of it.

The importance of rock wettability and interfacial tension in oil production has been discussed by several authors.[14,37] It has been found that the oil recovery from preferentially water-wet rock is significantly greater than those from preferentially oil-wet rock.[24,36] It has also been found that the wetting property of the reservoir rock is primarily determined by the natural surface-active substances in the reservoir fluids.[4] Thus, greater oil production

efficiency is expected by adding synthetic surface-active substances to control the reservoir wettability during a water flood.[44,50]

C. Capillary Pressure

The fundamental equation for the capillary pressure in a single straight capillary tube is given by

$$P_c = \frac{2\gamma_{wo}\cos\theta}{r} = \Delta\rho\gamma_{wo}gh \qquad (II-4)$$

where

P_c : $P_o - P_w$, capillary pressure, dynes/cm^2

$\Delta\rho$: $\rho_w - \rho_o$, gm/cc

r : radius of the capillary tube, cm

h : height of the water column, cm

Equation II - 4 states that the capillary pressure in this system is proportional to the adhesion tension and is inversely proprtional to the radius of the tube. It also states that the capillary pressure is proportional to the height of the column of water. The analogy with a bundle of capillaries has often been used in the study of a porous medium as the reservoir fluids exist in spaces which are capillary in size.

Leverett's[28] proposed J-function is a dimensionless function correlating the physical properties of the porous medium and the fluids with the capillary pressure in an

attempt to express capillary pressure data obtained from different samples in a generalized form:

$$J(S_w) = \frac{\Delta \rho g h}{\gamma} \sqrt{\frac{K}{\phi}} \qquad (II - 5)$$

Some investigators include contact angle in the J-function.[2]

$$J(S_w) = \frac{\Delta \rho g h}{\gamma \cos\theta} \sqrt{\frac{K}{\phi}} \qquad (II - 6)$$

Brown[7] has shown that the J-function gives a good correlation for the capillary pressure data obtained from unconsolidated sands and for the data obtained from the same formation. However, a poor correlation is attained for data obtained from different formations. Thus, he has suggested that the use of the J-function be restricted to specific lithologic types from the same formation.

A general expression for capillary pressure as a function of interfacial tension and curvature of the interface is due to Plateau:[39]

$$P_c = \gamma \left(\frac{1}{r_1} + \frac{1}{r_2}\right) \qquad (II - 7)$$

where r_1 and r_2 are principal radii of the interface curvature. It is apparent from Equation II - 7 that the smaller the radii of the interface curvature, the greater the

capillary pressure. Since the magnitude of the radii depends

on the texture of pores and the saturation of the fluids

present, it can be said that the specific pressure difference

across the interface may be given by a certain relative

saturation of the fluids present in the space. That is to

say, the capillary pressure can be expressed as a function of

saturation.

D. <u>Saturation History</u>

It has been known that the capillary pressure for

a porous medium is not single-valued. There is a significant

difference between the drainage and the imbibition capillary

pressure for the same system. McCardell[32] has explained

this phenomenon using a capillary system whose diameter

changes from small to large to small. From this analysis

he has shown that the wetting fluid saturation from the drainage

process is considerably higher than that from the imbibition

process when both capillary pressures are the same. It is

thus concluded that the capillary pressure-saturation

relationship is dependent on (1) the textural properties

of the pores, (2) physical properties of the fluids and the

solid, i.e. wettability of the solid and the interfacial

tension between the fluids, and (3) the history of the

saturation process.

E. Methods of Measuring Capillary
   Pressure on a Small Core Sample

Leverett[28] was the first investigator who
conducted a capillary pressure experiment on a porous medium.
His experiment was done on an unconsolidated sand pack by
"height-saturation method". The principle of this method is
to let wetting and non-wetting phases come to equilibrium
in a vertical sand column and measure resultant saturation
at a number of heights. The experiment was done in such a
manner that drainage and imbibition capillary pressure
curves were defined.

The height-saturation method, however, requires a very
long sample. Since naturally-occurring rock samples available
for laboratory experiments are usually small, this method is
not appropriate for such samples. For small core samples,
four basic methods have been devised. These methods are
(1) membrane method, (2) the mercury injection method, (3) the
centrifuge method, and (4) the dynamic method. These methods
are described and discussed in this section.

1. Membrane Method

Welge[51] proposed the use of a semi-permeable
membrane for measuring the capillary pressure. A membrane
is selected with uniformly distributed pores of such size that
the displacement pressure of the membrane for the selected
displacing fluid is greater than some predetermined maximum

pressure of investigation. The membrane is then saturated with the displaced fluid. Then some porous material (tissue paper, fine powder, etc.) saturated with the displaced fluid is placed on the membrane. This porous material ensures the phase continuity between the displaced fluid in the core and that in the membrane. The sample is then placed on top of the porous material. The displacing fluid is confined above the membrane and surrounds the sample. The pressure is applied to the displacing fluid in a stepwise fashion with small increments, and at every pressure the system is allowed to approach a static capillary equilibrium. As the pressure increases, a portion of the displaced fluid is expelled from the sample through the membrane and the volume displaced is recorded to determine the saturation. Thus, a relationship between saturation and the capillary pressure can be obtained.

Fritted glass disks,[9,12,33] porcelain,[49] cellophane,[43] among others, have been used successfully as the semi-permeable membrane. The maximum pressure that can be applied to this system is the displacement pressure of the membrane. Due to the limitation of the membrane material available, the maximum pressure is not more than 100 psi so far as is known.[7]

A different method has been devised by Hassler and Brunner[16] using the same principle. In their technique, vacuum is used rather than pressure. The wetting fluid is

withdrawn from the sample through a membrane by vacuum.

Among existing methods, the membrane method is considered to reproduce most accurately the capillary displacement in the reservoir. This is so because of the slowness of the approach to capillary equilibrium and because any combination of fluids may be used with the membrane method. The latter point is especially a marked advantage as it has been recognized that the use of reservoir-like fluids is preferred because the properties of pore space are related to the physico-chemical properties of reservoir fluids. This method, therefore, is considered to be the standard technique against which results from other methods are compared. The disadvantage of this method is the relatively slow approach to static capillary equilibrium after pressure has been applied.[2] Complete determination of a capillary pressure curve may take weeks.

2. Mercury Injection Method

Mercury injection method was originally devised as a pressure porosimeter by Drake and Ritter[41,42] to measure the pore size distribution of catalysts, and was modified by Purcell[40] for the determination of the capillary pressure of porous material. Purcell's equipment essentially consists of a fixed-volume sample chamber and a mercury displacement pump.

The principle of this method is to inject mercury into

the sample under a number of successively greater gas pressures applied above the mercury. As the sample chamber has a fixed volume, the amount of mercury injected into the sample at each pressure applied is equivalent to the volume of mercury added to the system by means of the mercury displacement pump. Thus, with the knowledge of the total pore volume of the sample, the mercury saturation can be calculated, and a capillary pressure curve is obtained. It is necessary, however, to correct the results as the cell expands and mercury compresses at high pressure.

In this system, the mixture of mercury vapor and residual air is the wetting phase, and the mercury the non-wetting phase. In order to correlate the results from this method to those from the membrane method, Purcell[40] has suggested a constant conversion factor independent of the character of the reservoir. The factor is calculated by analogy to capillary tubes and by assuming constant surface tensions and contact angles of mercury and water. The factor is

$$\frac{P_{cHg}}{P_{cw}} = \frac{\gamma_{Hg} \cos \theta_{Hg}}{\gamma_w \cos \theta_w} = 5 \qquad (II - 8)$$

where

P_{CHg}, P_{CW} : mercury and water-air capillary pressures, respectively.

γ_{Hg} : surface tension of mercury, = 480 dynes/cm

γ_W : surface tension of water, = 70 dynes/cm

θ_{Hg} : contact angle of mercury, = 140°

θ_W : contact angle of water, = 0°

The contact angle and the surface tension of mercury used in Equation II - 8 were obtained by Drake and Ritter[42] by averaging the values obtained on a large variety of solid materials.

There is, however, some doubt as to the validity of Purcell's assumptions. Henderson[21] has shown that the surface tension of mercury varies with the curvature of the interface. Pickell, et al, have reported that mercury is not strongly non-wetting; rather, it partially wets the rock surface. These two reports suggest that Purcell's assumptions of constant contact angle and surface tension may not be valid.

There have been some modifications as to the conversion factor suggested. One author says that the factor should be calculated on the assumption that the mean curvature of an interface in rock is a unique function of fluid saturation.[2] In this case, the factor is

$$\frac{P_{cHg}}{P_{cw}} = \frac{\gamma_{Hg}}{R_t} \bigg/ \frac{\gamma_w}{R_t} = \frac{\gamma_{Hg}}{\gamma_w} = \frac{480}{70} = 6.87 \qquad (II - 9)$$

where

R_t : mean curvature of the interface

Dumore and Schols[15] have used Wenzel's roughness factor of 1.3 for the Bentheim sandstone-mercury-air system and have suggested that the apparent contact angle for this system can be assumed zero. This suggestion has also resulted in the conversion factor of 6.87. Brown[7] has suggested that Purcell's theoretical value for the factor, 5.25, is a limiting value and that a higher value should be used as the water surface is sensitive to contamination, making it quite possible that the figure 70 dynes/cm is a maximum. He used different conversion factors ranging from 5.4 to 8.3 and obtained excellent results.

Pickell[38] also suggests that there is a tendency particularly in shaly sands, for mercury residual saturations to be excessively high when high initial mercury saturations are used. This may suggest that different pore structure may result when mercury and its gas are substituted for the reservoir-like fluids, especially when a clay-like substance is present. Rose[40] suggests in his discussion on Purcell's method that hysteretic uncertainties may be encountered when this method is used for the study of imbibition unless the porous medium is inert. This is to say, in the case of

an inert porous medium the character of the interstitial
spaces is unrelated to the physico-chemical properties of
the saturating fluids.

The advantages and disadvantages of this method may
be summarized as follows. The advantages of this method
are (1) the method is applicable to small, irregularly
shaped samples, (2) a complete capillary pressure curve can
be obtained in 30 to 60 minutes, and (3) the range of
pressure is 5 to 10 times that of the membrane method. The
disadvantage is the permanent loss of the sample due to the
unrecoverable mercury.

3. The Dynamic Method

The dynamic method was devised by Hassler[18] for
relative permeability studies and was modified by Brown[7]
for the determination of dynamic capillary pressure. The
apparatus consists of two semi-permeable membranes, one at
each end of the sample, and completely separate flow systems
for the two phases involved.

Brown has used gas as the non-wetting and oil as
wetting fluid. The membranes are saturated with wetting
fluid and are placed in the apparatus at each end of the
core. The phase continuity of the oil in the core and mem-
branes is established by some porous material placed between
the membranes and the core. The oil enters and leaves the
core through the membranes, and gas through the grooves in

the faces of them. The central part of each membrane is isolated from the other part for the determination of oil pressure. The difference between the pressures in oil and gas at the inflow end is the capillary pressure. The fluids pass through the sample at such a rate that the pressure drop in the two phases across the core is equal. This is accomplished by adjusting the gas flow rate. Thus, simultaneous steady-state flow of two fluids can be established by regulating the quantity of each fluid entering the core, and a complete capillary pressure curve can be obtained.

There have been several modifications of this method made by various investigators. Brownscombe,[8] et al., permitted counter flow, but experienced plugging of the sample. Care must be taken, therefore, to avoid possible plugging and the distortion of the sample in this system. Leas,[27] et al., eliminated the use of the outlet end disk and permitted gas flow while liquid saturation remained constant in the core. Although there still remains some uncertainty as to the fundamental difference between the static and the dynamic capillary equilibrium, Brown's investigation shows good agreement between the data obtained from this method and the membrane method for a limestone and a sandstone in an oil-gas system.

The advantages and disadvantages for this method may be summarized as follows. The advantages are (1) capillary

pressure is equal throughout the core, thus the fluid
saturation is also uniform provided the core is homogeneous,
and (2) the end effect can be eliminated, as the capillary
pressure is equal at both ends of the core. These two
points result in a marked advantage for this method,
namely that (3) the direct measurement of saturation and the
capillary pressure is possible, while in other methods only
average saturation and the capillary pressure at a certain
cross-section of the sample are obtained. The disadvantages
are (1) relatively slow approach to capillary equilibrium as
in the membrane method, and (2) the difference between
dynamic and static capillary equilibrium has not been fully
appreciated.

4. The Centrifuge Method

Hassler and Brunner[19] have reported the application
of a centrifuge for measuring the capillary pressure on a
small core sample. This method has been used by a number
of investigators [14,26,31,46] for capillary pressure,
connate water saturation, and wettability studies.

The centrifuge method makes use of a greatly
increased drainage effect by submitting the saturated cores
to an increased gravitational force created by the high
normal component of centrifugal acceleration. The sample to
be tested is rotated at a number of successively greater
speeds, the speed being held constant until the capillary

equilibrium i██████████ach speed chosen. The sample
holder is ████████████ way that the amount of fluid
displaced is █████████ pipette and can be read by the
operator with the aid of a stroboscope. The average satura-
tion of the sample can thus be determined with the knowledge
of the total pore volume. The speed of rotation is converted
into a suitable force unit, thus a complete capillary
pressure curve can be obtained. The capillary pressure
curves obtained by the centrifugal method, however, are not
a complete description of the capillary pressure versus
saturation relationship in a porous medium, for the procedure
does not measure directly either the saturation or the
capillary pressure.

The basic theory for the computation of the capillary
pressure has been shown accurately by Hassler.[19] If a
cylindrical core of length L, containing a liquid of density
ρ is subjected to an acceleration g, and if the capillary
pressure at the outer end of the core is zero, then
the capillary pressure at height h above the lower
end of the core will be $\rho g h$. Since the capillary pressure
can be considered as a function of saturation, fluid satura-
tion, conversely, can be expressed as a function of the
capillary pressure. By definition, the average saturation
obtained by this method is given by

$$\bar{S} = \frac{1}{L} \int_0^L S(\rho g h) \, dh \qquad (II - 10)$$

If we define the capillary pressure at the inner end of the core (closer to rotary axis) as Z and at any point in the core as x, Equation II - 10 can be simplified as

$$z\overline{S} = \int_{0}^{Z} S(x)\ dx \qquad (II - 11)$$

where

$$x = \rho g h$$

and

$$Z = \rho g L$$

From Equation II -11, it follows that

$$s(\blacksquare) = \frac{d}{d\blacksquare}\ (z\overline{S}) \qquad (II - 12)$$

The saturation for capillary pressure Z can thus be obtained by graphical differentiation of the curve $z\overline{S}$ versus Z.

The centrifugal acceleration, however, is proportional to the distance from the centre of rotation, and will change along the length of the sample. Thus, the equivalent equation to Equation II - 11 for the centrifugal field is more complicated. It is given by Equation II - 13:

$$z\bar{S} = \cos^2\frac{\alpha}{2} \int_0^z \frac{S(x)' \, dx}{\sqrt{1 - \frac{x}{z}\sin^2\alpha}} \qquad (II - 13)$$

where

$$z = \frac{\rho}{2} \, \omega^2 (r_2^2 - r_1^2)$$

$$x = \frac{\rho}{2} \, \omega^2 (r_2^2 - r^2)$$

$$\cos \alpha = r_1/r_2$$

The solution of equation II - 13 for S(x) involves very tedious successive approximations. Hassler[19] has suggested, however, that a constant acceleration can be used along the core without introducing serious error provided the ratio r_1/r_2 is sufficiently large. If such is the case, Equation II - 12 can be used to determine saturation. He suggested the minimum value for cos α to be 0.7. Slobod, et al., have used the average acceleration measured at the centre of the core and cos α as 0.85. The capillary pressure in psi at height h in the core at speed n (rpm) with the average radius of rotation $\bar{r}$ is then given by the following equation:

$$P_c = 1.578 \times 10^{-7} \rho \, n^2 \, \bar{r} \, h \qquad (II - 14)$$

Szabo[47] has devised a technique for measuring imbibition capillary pressure in a centrifuge. A sample having a water saturation close to the connate water saturation is placed in the imbibition cell, and then a semi-permeable membrane permeable only to water is placed on the face of the inner end of the core. After the continuity of water in the core, membrane, and the water reservoir located on the opposite side of the membrane is ensured, the cell is filled with oil. The centrifuge is then started at a speed less than the maximum attained during the displacement test. After the capillary equilibrium is reached, the centrifuge is stopped to determine the saturation by weighing the sample.

While imbibition takes place against gravitational acceleration in the membrane method, in Szabo's method, the centrifugal acceleration works in favour of imbibition. Szabo also assumes that significant re-distribution of fluids in the core does not occur while the centrifuge is stopped for the determination of saturation.

Hoffman[22] has reported that the time required for determining the capillary pressure can be further reduced by using a constantly-accelerated centrifuge. A centrifuge with a speed control system for increasing centrifuge speed at a constant rate is used in his study. Centrifuge speed, average saturation, and capillary pressure are expressed as a function of time, and by proper rearrangement

of Hassler's equation, saturation at the end of the core
closer to the rotary axis can be evaluated at a given time.
A complete capillary pressure curve can be obtained in
approximately 6 hours by this method, while Hassler's equip-
ment requires at least twice as much time as Hoffman's.

The advantages for the centrifuge method are (1) the
greatly reduced time required for obtaining a complete capil-
lary pressure curve, and (2) high capillary pressure created
by proper design of the equipment. The disadvantages for
this method are that (1) the capillary pressure-saturation
relationship cannot be obtained directly, and that (2) the
imbibition curve for pressures greater than zero and the
drainage curve for pressures less than zero cannot be
obtained by this technique.

CHAPTER III

A CAPILLARY PRESSURE MODEL AS A

FUNCTION OF SATURATION

A. Capillary Pressure Model

In order to carry out the analysis, an assumption was made that the capillary pressure can be regarded as the independent variable which determines the saturation at a given cross-section within a porous medium. It was also assumed that the porous medium is homogeneous. The functional relationship between the capillary pressure and saturation was such that it meets the following criteria:

(1) The area under the capillary pressure versus saturation curve must be finite, as the area represents the work done in creating a new boundary surface.[28]

(2) The capillary pressure is finite near $S_w = 1$.

(3) The slope of the capillary pressure curve near $S_w = S_{wi}$ approaches minus infinity.

(4) Any functional relationship must agree with experimental evidence.

Generally, two types of drainage capillary pressure curves are found among the existing data. Curve 1 in Figure III - 1 is believed to represent the typical capillary pressure curve of a very thin porous disk,[48] while curve 2

24
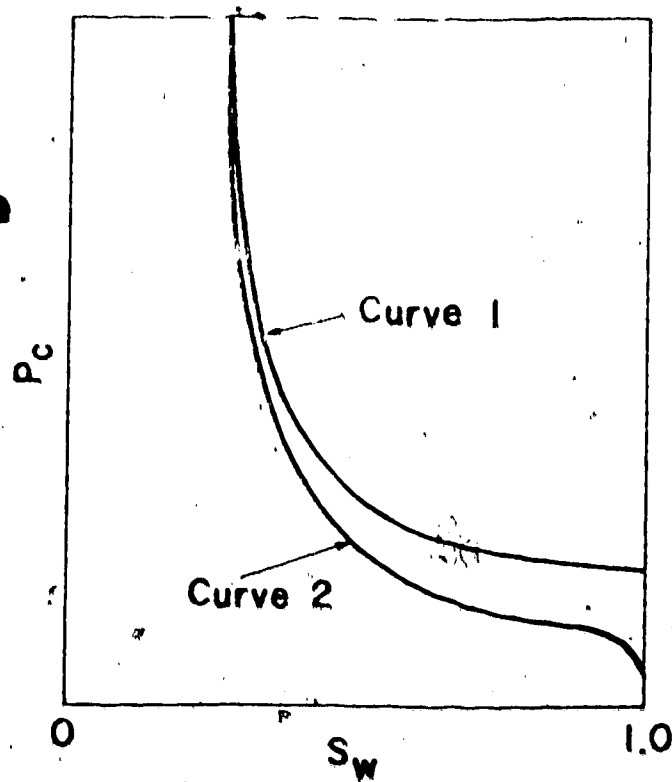
Figure III - 1

Typical Capillary Pressure Curve

is often obtained in laboratory measurements. Note that there is a discrepancy between the two curves in the region near $S_w = 1$. In this region, curve 2 shows inflection, while curve 1 does not. It is believed that for a homogeneous porous medium, the capillary pressure curve would behave like curve 1, as the slope of the curve during drainage is a measure of the pore size distribution. The more uniform the pore size, the more nearly horizontal or the flatter the capillary pressure curve.[13]

It should also be pointed out that the capillary pressure data obtained using the membrane method have often been misinterpreted. The results obtained from this method do not represent the true capillary pressure versus saturation relationship; rather, they represent the relationship between the capillary pressure at a particular cross-section of the sample versus average saturation. Thus, serious error may result in determining displacement pressure and both saturation and capillary pressure in the relatively low pressure region.

Therefore, it seems reasonable to select curve 1 in Figure III - 1 as the basis for a capillary pressure model. It is also believed that this type of curve can model data from naturally occurring rock samples, for the data in the region near $S_w = 1$ usually have little practical importance for most engineering purposes.

B. Construction of the Model

It is generally accepted that the capillary pressure curve is discontinuous at the displacement pressure, P_d, below which saturation is unity. It is also generally accepted that there exists some minimum wetting phase saturation for a porous medium. Therefore, it seems reasonable to consider the domains of the capillary pressure and saturation as given below in order to describe the continuous portion of the curve mathematically:

$$P_d \leq P_c < \infty$$

and

$$S_{wi} \leq S_w \leq 1$$

The displacement pressure and the connate water saturation, S_{wi}, are believed to be unique characteristics for a system of a given combination of fluids and solids.[20]

Fayer and Sheldon[16] have suggested that, for a water-wet medium, the slope of the capillary pressure curve approaches minus infinity as saturation S decreases to zero, where

$$S = \frac{S_w - S_{wi}}{1 - S_{wi} - S_{or}} \qquad (III.-1)$$

This is consistent with their condition that dP_c/dS should behave like $1/S$ near S equal to zero. On this basis it seems reasonable to postulate that

$$\frac{dP_c}{dS} = -\frac{1}{S} \qquad (III - 2)$$

which, upon integration, yields

$$P_c = -\ln S + P_d \qquad (III - 3)$$

The capillary pressure may be normalized by defining

$$\pi_c = \frac{P_c - P_d}{\sigma} \qquad (IV - 4)$$

where σ is the normalizing parameter for capillary pressure which incorporates the effects of interfacial tension, wettability, and pore-size distribution. Both P_d and σ have to be determined experimentally.

The model now can be written as

$$S_w = S_{wi} + (1 - S_{wi}) \exp\left(-\frac{P_c - P_d}{\sigma}\right) \qquad (III - 5)$$

and the normalized form of the model is given by

$$\pi_c = -\ln S \qquad (III - 6)$$

C. Application of the Proposed Model to the Data Obtained Using the Centrifuge

The proposed capillary pressure model (Equation III - 5) has to be modified in such a way that the data obtained using the centrifuge (i.e., average saturation and rotation speed) can be used. The centrifugal acceleration is defined by

$$\alpha = r\omega^2 \qquad\qquad (III - 7)$$

The capillary pressure in centrifugal acceleration is given by

$$P_c = \Delta\rho\omega^2 \ (R - h/2)h \qquad\qquad (III - 8)$$

Note that it is assumed that the capillary pressure at the outer end of the core is zero. This assumption is justified by the good agreement between the results obtained using the membrane and the centrifuge methods.[19] The capillary pressure profile within the core is shown in Figure III - 2.

By definition, the average saturation of the core is

$$\bar{S}_w = \frac{1}{H} \int_0^H S_{wi} + (1 - S_{wi}) \ \exp(-\frac{P_c - P_d}{\sigma}) \ dh$$

$$(III - 9)$$

At some critical rotation speed, ω_c, the capillary pressure at the outer end of the core reaches the displacement pressure. Until such rotation speed is reached, the water saturation remains unity. After the critical rotation speed is exceeded, the location at which $P_c = P_d$ is assumed to move along the core and to approach $h = 0$.

The displacement pressure is a unique property of the porous medium, and has only one value for any particular specimen.[20] Its value is a measure of the degree of rock wettability, the oil -water interfacial tension, and the diameter of the largest pore on the exterior of the rock sample. Therefore, if the largest pore size is uniformly distributed throughout the core, as it is expected to be in a homogeneous porous medium, the above assumption should be valid. Figure III - 3 shows the saturation profile in the core for some $\omega > \omega_c$, where $h*$ is the location in the core at which $P_c = P_d$ for any $\omega > \omega_c$.

From the derivation cited in Appendix A, the following expression results:

$$\bar{S}_w = S_{wi} + \frac{(1 - S_{wi})h*}{H} + \frac{(1 - S_{wi})}{\Delta\rho\omega^2 H} \int_{P_d}^{Z} \frac{\exp(\frac{P_c - P_d}{\sigma})\,dP_c}{\sqrt{R^2 - \frac{P_c(2R-H)H}{Z}}}$$

(III - 10)
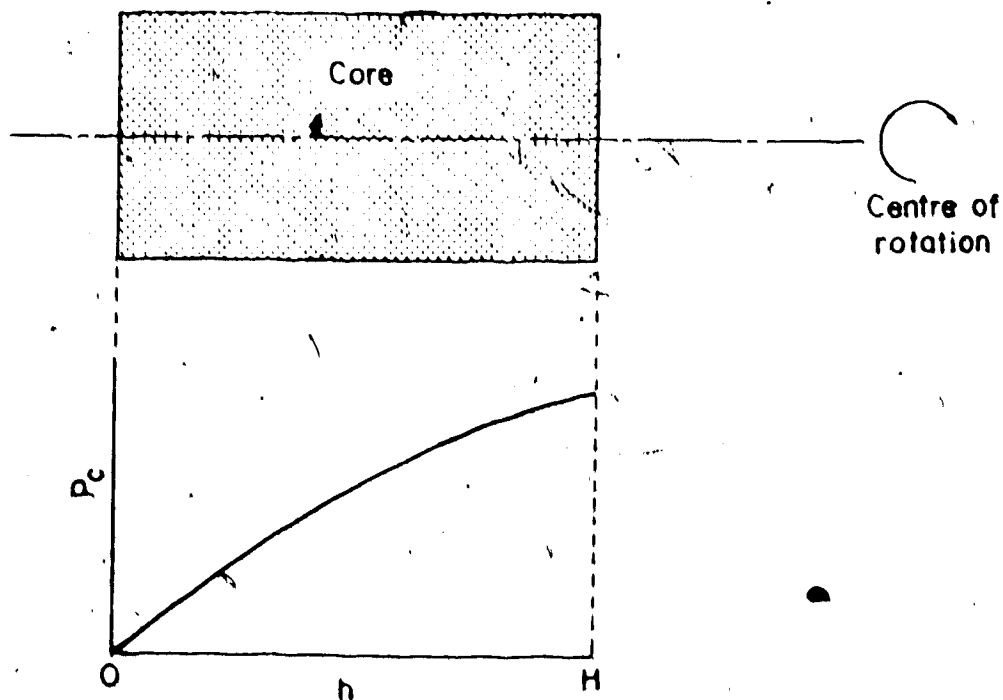
Figure III - 2

Capillary Pressure Profile Within a Porous

Medium Being Rotated in a Centrifuge
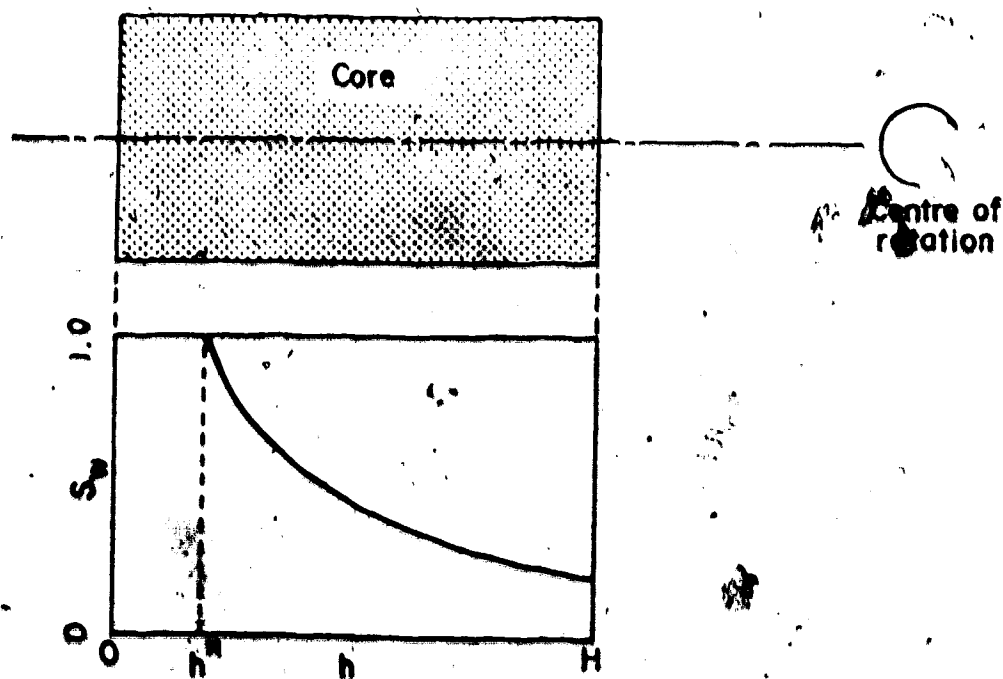
Figure III - 3

Saturation Profile Within a Porous Medium

Being Rotated in a Centrifuge

or,

$$\overline{S_w} = S_{wi} + \frac{(1-S_{wi})\ (R-\frac{H}{2})\,P_d}{(R-\frac{h^*}{2})\,Z} + \frac{(1-S_{wi})\ (R-\frac{H}{2})}{Z}$$

$$\times \int_{P_d}^{Z} \frac{\exp\ (-\dfrac{P_c - P_d}{\sigma})\,dP_c}{\sqrt{R^2 - \dfrac{P_c\,(2R - H)\,H}{Z}}} \qquad (III - 11)$$

Equation III - 11 could not be solved analytically; therefore, two methods were employed to solve the equation, i.e.

(1) Numerical Integration Method

(2) Approximation Method

The denominator within the integral sign of Equation III - 11 behaves in a linear fashion in the integral limits. Thus, the midpoint may be used to approximate this term, or

$$\frac{1}{2}\left[\sqrt{R^2 - (2R-H)\,H\frac{Z}{Z}} + \sqrt{R^2 - (2R-H)\,H\frac{P_d}{Z}}\right] = R - \frac{H+h^*}{2}$$

Substitution of the above and integration of the Equation III - 11 results in:

$$\overline{S_w} = S_{wi} + \frac{\sigma(1-S_{wi})(R-\frac{H}{2})}{(R-\frac{H+h^*}{2})Z}\left[\frac{R-\frac{H+h^*}{2}}{R-\frac{h^*}{2}}\frac{P_d}{\sigma}\right.$$

$$\left. +1 - \exp(-\frac{Z-P_d}{\sigma})\right] \qquad (III - 12)$$

Note that from Equation III - 8

$$h^* = R - \sqrt{R^2 - \frac{2 P_d}{\Delta\rho\omega^2}} \qquad (III - 13)$$

The above equation was used as the Approximation Method.

CHAPTER IV

EXPERIMENTAL APPARATUS AND PROCEDURE

In order that the capillary pressure in a porous medium be examined experimentally, a total of six sandstone cores were obtained from the Department of Chemical and Petroleum Engineering, the University of Alberta. These samples were about one inch in diameter and between one and one and a half inches in length.

Prior to the capillary pressure tests, the porosity and the permeability of the samples were determined using a specially constructed Boyle's law porosimeter and a liquid permeameter. The porosimeter consisted of a core holder and an expansion chamber connected to a gas supply and a vacuum pump as shown schematically in Figure IV - 1. By calibrating with aluminum cylindrical blanks of known solid volume, the matrix-volume of the cores was determined and porosity determined. The permeameter consisted of a core holder, liquid injection piston, flow-rate regulator, and a precision-bore capillary tube for flow-rate measurement. The permeameter is shown schematically in Figure IV - 2. The samples were saturated with the wetting fluid using a core saturator shown schematically in Figure IV - 3.

A. Drainage Capillary Pressure Cell

Two capillary pressure cells were constructed for the

34

Figure IV - 1   Schematic Layout of Boyle's Law Porosimeter
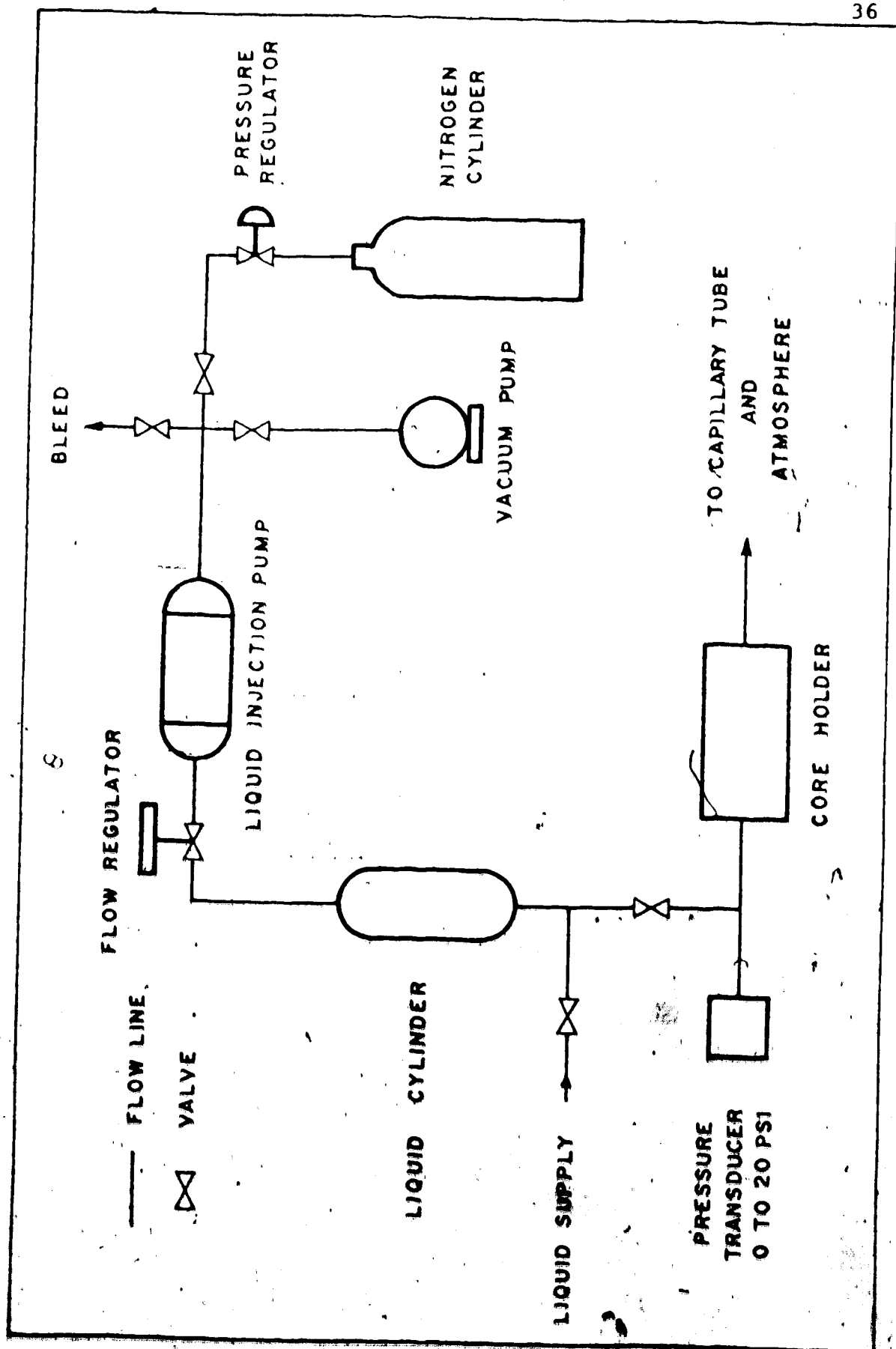
Figure IV – 2   Schematic Layout of Liquid Permeameter
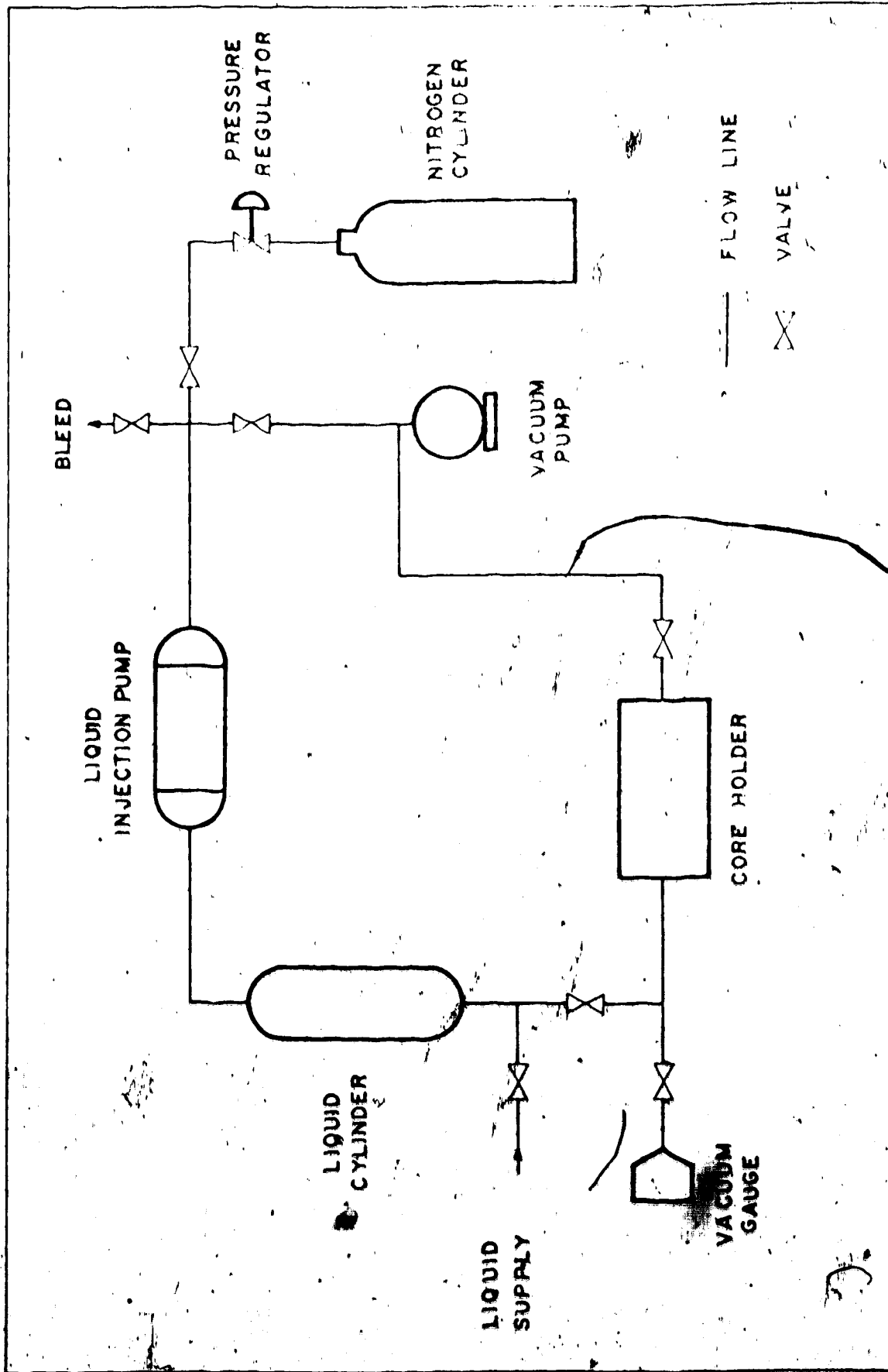
Figure IV. – 3 Schematic Layout of Core Saturator

determination of the drainage capillary pressure on a small core sample in the centrifuge. The centrifuge method was chosen primarily for the reduced time required to obtain data and for its reliability and good reproducibility. Initially, the membrane method was considered for use along with the centrifuge method, but due to unavailability of membrane material with suitable pore size, the membrane method was abandoned and only the centrifuge cell was constructed. A semi-permeable membrane was considered for use in the centrifuge cell, but this design was abandoned for the same reason and the cell was constructed without a membrane. Figure IV - 4 shows the cross-section of the cell in actual dimension. The cell consisted of a core holder and a pipette for determining the volume of displaced fluid. A 3/8 inch diameter precision-bore (I.D. tolerence ± 0.0004 inch) glass tube was used as the pipette.

The core holder body was made of anodized aluminum, while the core support disk and the bottom cap were made of stainless steel. The arm and the tube body were made of mild steel, in order to locate properly the centre of weight. A stainless steel coil spring was placed in the core holder to stabilize the sample.

B. The Apparatus Assembly

An International Model U centrifuge was used in this work, operating at various speeds up to 2,200 rpm with a Model
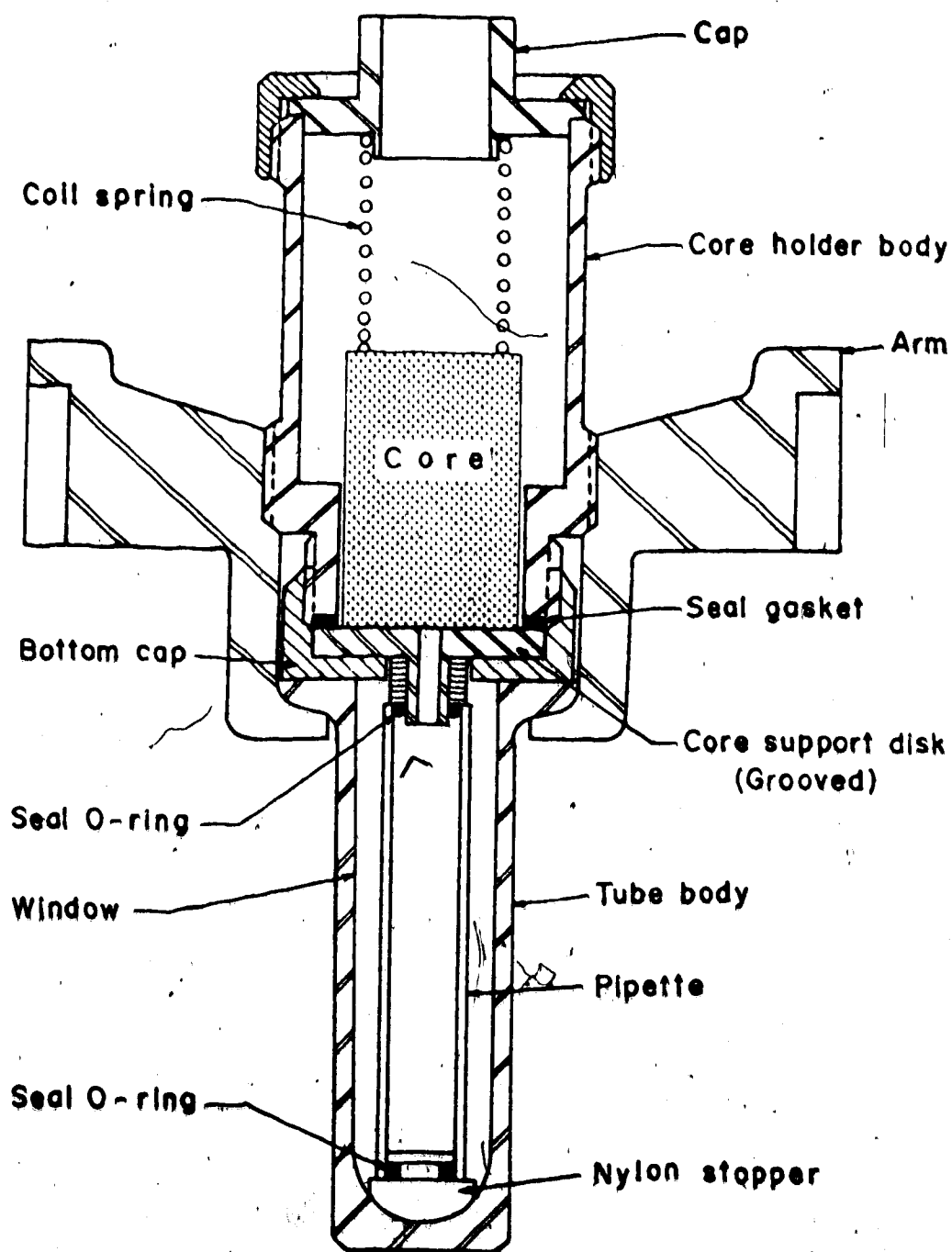
Figure IV - 4

Drainage Capillary Pressure Cell

976 centrifuge head (Trunnion, 4 place). A window was provided on the lid of the centrifuge to facilitate observation of the drainage cell with the aid of a calibrated stroboscope (1540-P1-General Radio).

After capillary equilibrium was reached at each centrifuge speed selected, the water volume displaced from the core was recorded by means of a camera (Miranda 85 mm, F 3.5) using high speed film (Tri-X, ASA 400). The same stroboscope was used to provide a light source for photography and to determine the speed of the centrifuge.

C. Experimental Procedure

1. Preparation of Sample

The dimensions of the samples were obtained by taking the average of ten caliper measurements, and the bulk volume determined. Prior to tests, the samples were cleaned in a soxhlet extractor[2], for 24 hours with CCl_4, dried at 95° C for 24 hours, then heated at 500°C for 10 hours to remove organic material from the surface. This treatment is believed to render the samples strongly water-wet.[11] After the samples were cooled in a desiccator, porosity was determined by Boyle's law porosimeter using nitrogen.

Dow Corning 200 Fluid (1.5. cs) was selected as the non-wetting phase for its chemical stability and purity, and 5% brine was selected as the wetting phase for its similarity to reservoir water.[49] The densities and the viscosities of the wetting and non-wetting fluids and the interfacial

tension between them were obtained at 20°C at the Standards Laboratory, Department of Chemical and Petroleum Engineering, the University of Alberta.

In order to saturate the samples, they were placed in the core saturator and kept under vacuum at 10μHg for 24 hours, then saturated with 5% brine. Liquid permeability was then measured using the permeameter described earlier.

2. Capillary Pressure Determination

After the capillary pressure cell was assembled, a small amount of brine mixed with uraine dye was injected into the pipette using a hypodermic syringe to establish the initial brine level. The cell was then filled with oil, leaving sufficient space for the sample to be tested. The sample, after having excessive brine blotted from its surface, was immersed in the oil and placed on the support disk in the cell. A stainless steel coil spring was used to stabilize the sample in position. Both centrifuge cells were prepared in this manner and the weight of both cells was made identical in order to minimize centrifuge vibration.

The initial oil-water interface level was recorded with the camera, then the cells were placed in the centrifuge on opposite sides of the rotation axis from each other and the centrifuge started. The speed was held constant at a number of successively greater speeds until capillary

equilibrium was reached. The equilibrium was normally obtained in 30 minutes to 3 hours depending on the sample and the centrifuge speed. The stroboscope was used to determine the speed of the centrifuge and to provide a source of light for photography. The uraine dye, being fluorescent, made the interface clearly visible and improved photography. Care was taken especially to maintain constant centrifuge speed, as the fluids in the core tend to re-distribute if the speed fluctuates. After the measurement was completed, the centrifuge was stopped and the remaining brine was extracted from the sample using a soxhlet extractor for the material balance check.

3. Determination of Average Saturation and the Capillary Pressure

Photographs were printed magnifying the pipette to approximately three times its size. With the aid of reference lines provided on the pipette, the oil-water interface level was determined with calipers and the volume of brine displaced from the sample obtained, from which the average water saturation could be readily calculated.

The capillary pressure at the inner end of the sample was determined using the following equation: [46]

$$P_c = 1.578 \times 10^{-7} \Delta\rho \; n^2 (R - H/2)H \qquad (IV - 1)$$

The distance from the centre of rotation to the outer face

of the core (or to the core-support disk) in this experiment was measured to be 16.314 cm.

4. Treatment of Data

Equations III - 11 and III - 12 were employed to calculate the true water saturation at the inner end of the sample. An algorithm to perform a least-square estimation of non-linear parameters, developed by Marquardt,[30] was utilized to estimate the parameters S_{wi}, σ, and P_d. After the parameters were estimated, the capillary pressure model (Equation III - 3) was used to generate the capillary pressure curve. (See Figures V - 10 and V - 11)

CHAPTER V

RESULTS AND DISCUSSION

A. Testing of Model

In order to test the model, capillary pressure data were taken from Calhoun's[11] paper. His data were obtained for two silica core samples using the membrane method. The displacing and the displaced fluids used were air and water, respectively. The lengths of the samples were not given by Calhoun, and therefore were assumed to be 2.54 cm as this was the size commonly used in the membrane method.

Two approaches were employed to test the model: (1) by rearranging the model to interpret the data correctly and (2) by assuming that the membrane method results represent a true saturation versus capillary pressure relationship.

1. Approach 1

As is mentioned in a previous chapter, the membrane method results do not represent true saturation versus capillary pressure relationship due to gravity. Figure V - 1 - A is a simplified illustration of the membrane cell for an air-water system.

Air pressure P_g is recorded as the experimental capillary pressure. Note that P_g is the capillary pressure at $h = 0$. Due to gravity, the capillary pressure increases

(A)

Gas pressure

Core

Disk
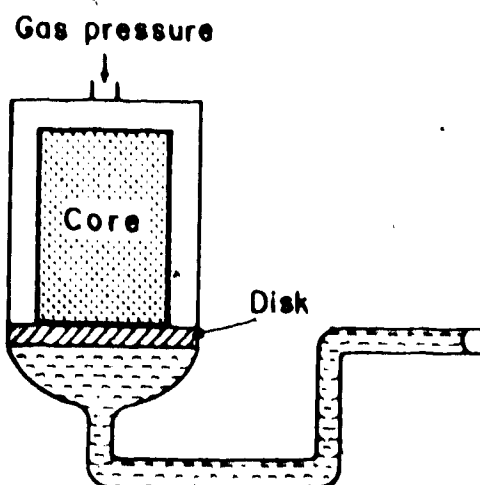
(B)
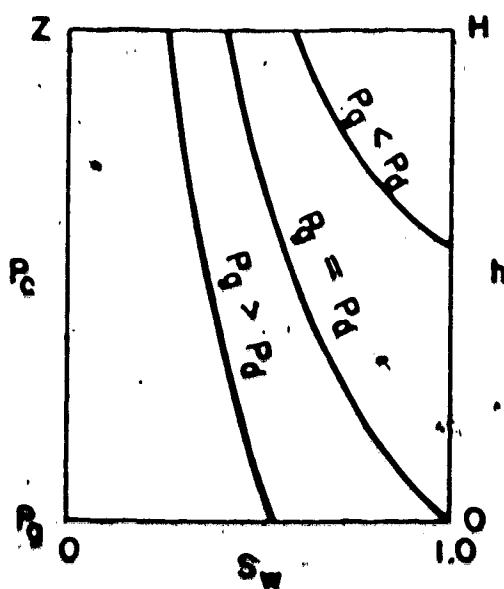
Figure V - 1

The Membrane Cell

with height to a maximum of $P_g + \rho_w gH$ ($=Z$) at $h = H$. Consequently, saturation also varies along the core as is shown in Figure V - 1 - B. The saturation determined experimentally is in fact an average saturation of the core.

It is necessary to alter the model so that average saturation $\overline{S_w}$ can be correlated to P_g. Equations V - 1 and V - 2 result from the required derivation given in Appendix B.

For air pressure $P_g \geq P_d$

$$\overline{S_w} = S_{wi} + \frac{\sigma(1-S_{wi})}{\rho_w gH} \left[\exp\left(-\frac{P_g-P_d}{\sigma}\right) - \exp\left(-\frac{Z-P_d}{\sigma}\right) \right]$$

$$(V - 1)$$

For $P_g \leq P_d \leq P_g + \rho_w gH$

$$\overline{S_w} = S_{wi} + \frac{1-S_{wi}}{\rho_w gH} \left[P_d - P_g + \sigma\left\{ 1-\exp\left(-\frac{Z-P_d}{\sigma}\right)\right\} \right]$$

$$(V - 2)$$

The initial displacement takes place when the capillary pressure at the top of the core, i.e. Z, reaches P_d.

The air pressure at this time will be $P_d - \rho_w gH$. It is for this reason that two equations are derived, one for $P_g \geq P_d$ and the other for $P_g \leq P_d$.

Using Equation V - 1 and the capillary pressure data for $P_g \geq P_d$, the parameters were estimated applying the Marquardt Algorithm. These parameters were used in the following manner:

(1) $\overline{S_w}$ versus P_g generated for $P_g \geq P_d$ using Equation V - 1

(2) $\overline{S_w}$ versus P_g generated for $P_g \leq P_d$ using Equation V - 2

A complete $\overline{S_w}$ versus P_g curve was obtained by combining the results. The solid curve (curve 1) in Figures V - 2 and V - 3 is the generated $\overline{S_w}$ versus P_g relationship for samples 2 - L and 3 - L, respectively.

It is seen that the model simulates the inflection of curvature for the relationship near $\overline{S_w} = 1$. This inflection is due to the fact that $\overline{S_w}$ is calculated rather than S_w. However, the greater degree of inflection in the experimental data indicates that it is influenced by other factors than just gravity, such as the pore-size distribution (i.e. existence of very large pores).

2. Approach 2

Here, the $\overline{S_w}$ versus P_g results were assumed to represent S_w versus P_c. The model (Equation III - 5) could readily

SAMPLE   2 - L

○   , Calhoun's data

———   Modeled curve 1

- - - -   Modeled curve 2

AIR PRESSURE P_a , cm Hg

AVERAGE WATER SATURATION $\overline{S_W}$
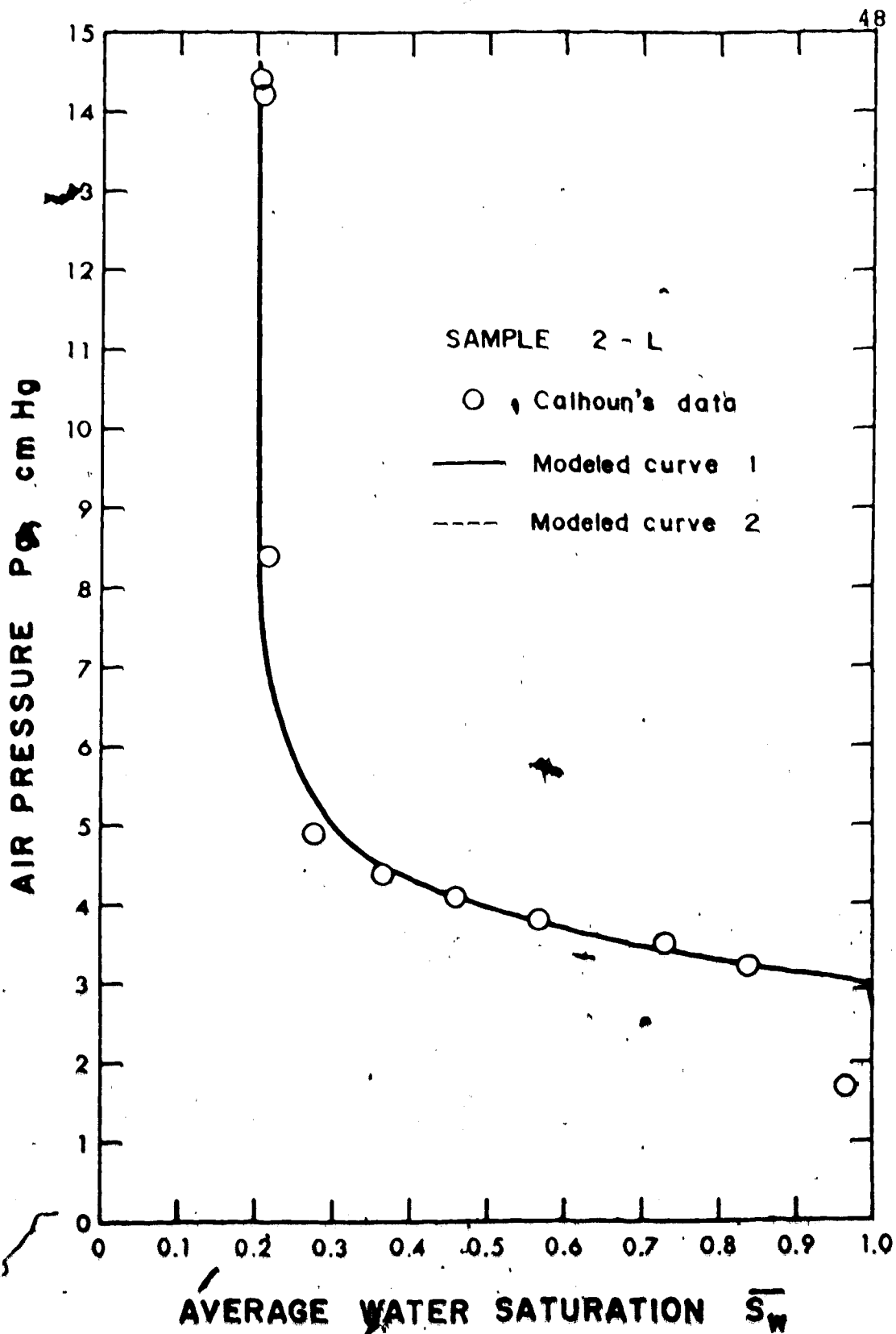
Figure V - 2

Calhoun's Data and the Modeled Curve
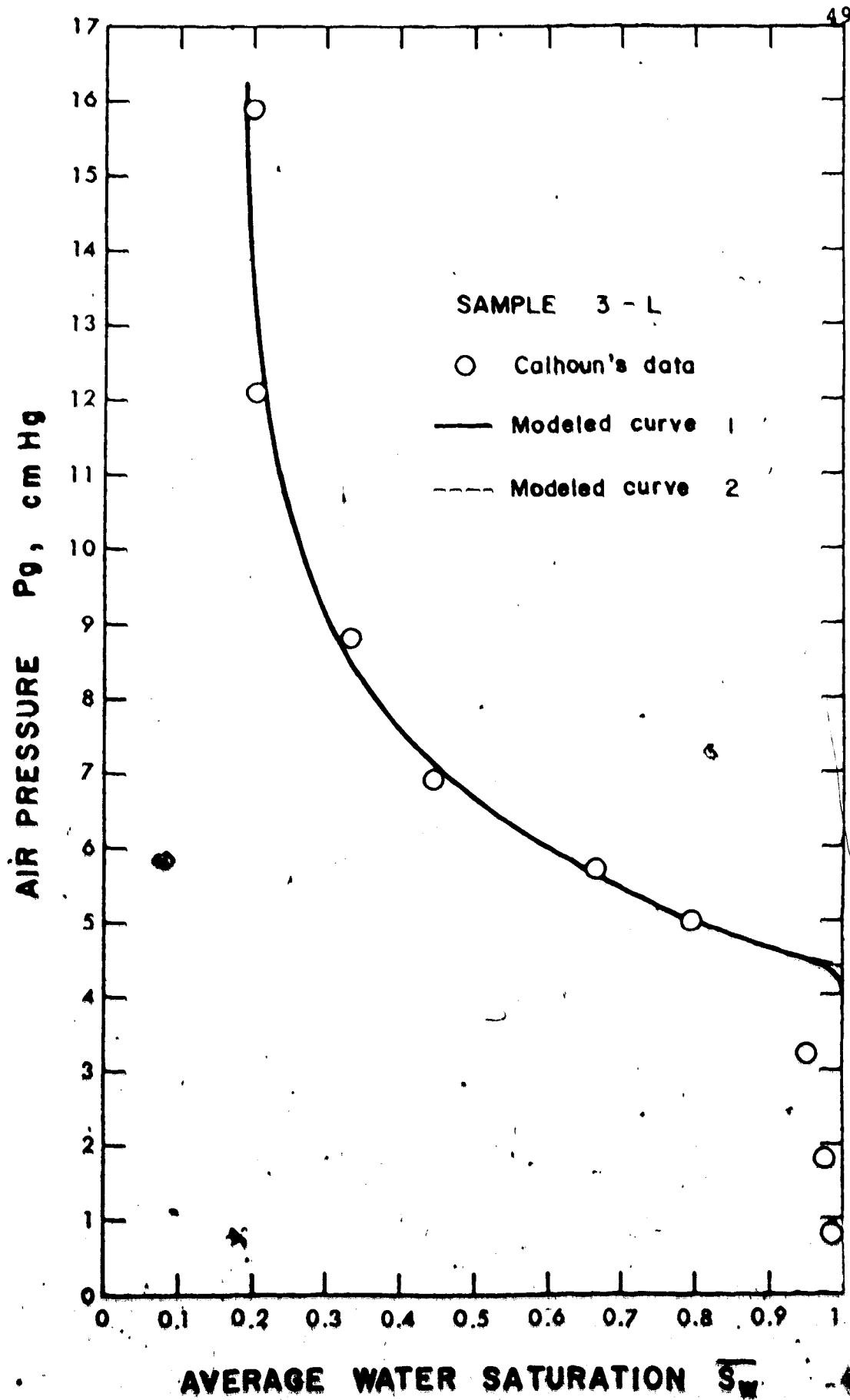
Figure V - 3   Calhoun's Data and the Modeled Curve

be used to estimate the parameters without any rearranging.

Using the data points for $P_g > P_d$, the parameters were estimated and the capillary pressure curve generated. Generated curves are given as the dotted line (curve 2) in Figures V - 2 and V - 3. It is to be noted that the solid curve in the region where $P_g \geq P_d$ represents generated data from both approaches.

3. Comparison of the Two Approaches

Excellent agreement is noted between curve 1 and 2 in Figures V - 2 and V - 3 and between the parameter values estimated (Table V - 1). Parameter values are in fact the same except at P_d, where this difference is within linear confidence limits. Separation of the two curves in the region $P_g \leq P_d$ is due to the neglect of gravity in the second approach. For the same reason, the P_d estimated in the first approach is greater than that in the second approach. The gas pressure P_g at $\overline{S_w} = 1$ obtained in the first approach is less than P_d by a constant amount of $\rho_w gH$.

The agreement between the two approaces justifies the assumption made in the second approach. This assumption, however, is not valid when the sample is relatively long. The agreement between the data and the modeled curve indicates that the lengths of the samples assumed are not unreasonable.

TABLE V - 1

PARAMETERS ESTIMATED USING CALHOUN'S DATA

| Sample | ± linear confidence limits | | | |
| | 2-L | | 3-L | |
	curve 1	curve 2	curve 1	curve 2
S_{wi}	0.2025 ± 0.0162	0.2025 ± 0.0162	0.1841 ± 0.0190	0.1841 ± 0.0190
σ	0.9326 ± 0.0838	0.9326 ± 0.0838	2.4604 ± 0.2594	2.4604 ± 0.2594
P_d	3.1217 ± 0.0445	3.0300 ± 0.0446	4.4092 ± 0.1172	4.3165 ± 0.1172

4. Dimensionless Capillary Pressure
   Curve and Conclusion

Calhoun obtained capillary pressure data on tetra-
decane-water and oleic-acid-water systems using the same
samples. In these systems, the gravity effect is smaller
than in the air-water combination because smaller density
differences exist between the fluids. Using the second
approach, parameters were obtained and then normalized capil-
lary pressure (Equation III - 4) and saturation (Equation
III - 1) were calculated using the data points for $P_g > P_d$.

The results shown in Figure V - 4 indicate that the
suggested model can be used effectively regardless of fluid
combination. The parameter σ seems to incorporate the effect
of interfacial tension, wettability, and the pore-size
distribution. With these results, it is concluded that the
model may be regarded as universal.

B. Results

1. Experimental Results

The physical properties of the samples are given in
Table V - 2. The samples are all sandstone and are approxi-
mately one inch in diameter and one and a half inches in
length. The porosities range between 15 and 24 percent while
permeabilities range between 30 and 430 millidarcies. The
properties of the fluids used are given in Table V - 3.

The experimental data $\bar{S}_w$ and Z for each sample are
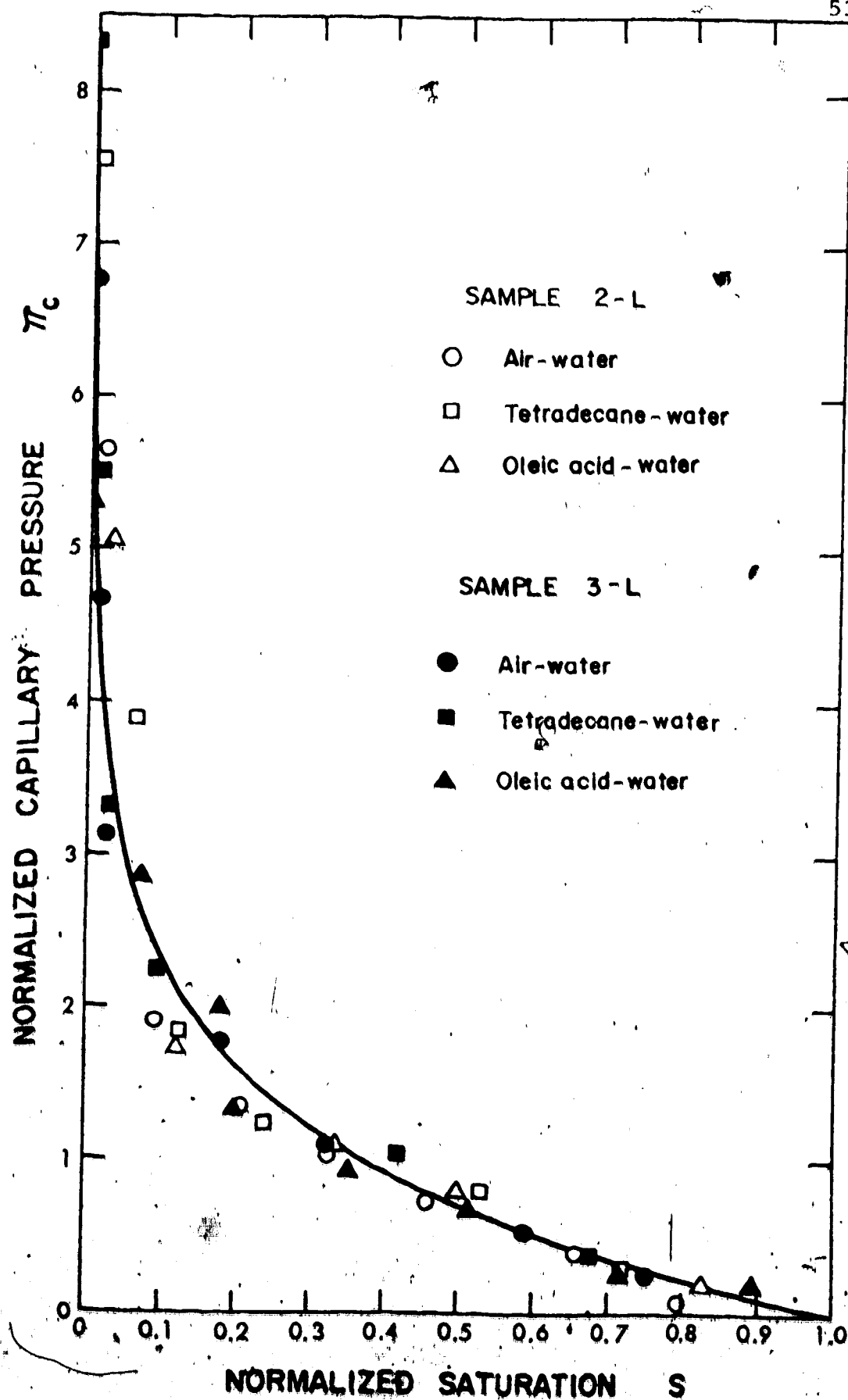
Figure V - 4   Dimensionless Capillary Pressure Curve

TABLE V - 2

PHYSICAL PROPERTIES OF THE SAMPLES

Sample	A	B	C	D	E	F
Diameter (cm)	2.446	2.443	2.449	2.456	2.532	2.535
Length (cm)	3.846	3.861	3.843	3.810	2.449	3.434
Bulk Volume (cm^3)	18.35	18.55	18.15	18.05	12.33	17.33
Pore Volume (cm^3)	3.89	4.03	4.29	3.52	2.44	2.70
Porosity	0.215	0.223	0.237	0.195	0.198	0.156
Liq. Permeability (md)	253	255	429	146	400	30

TABLE V - 3

PHYSICAL PROPERTIES OF THE FLUIDS

AT $20.0 \pm 0.02°C$

	Density (g/cm^3)	Viscosity (cp)
5% Brine	1.0365	1.0784
Dow Corning 200 Fluid	0.8475	1.4194
Difference in Densities	0.1890	
Interfacial Tension between the Fluids		37.47 dynes/cm

tabulated in Tables C - 1 through C - 6 in Appendix C and are plotted in Figures V - 5 through V - 10. Three duplicate experimental runs were made on samples A, B, and C, and two runs were made on the other samples.

During the experiments, no shifting of the centre of rotation or irregular vibration was observed in the centrifuge. The temperature in the centrifuge did not exceed the room temperature by more than 5°C, therefore the properties of the fluids were assumed to remain constant.

The maximum time required for the samples to come to equilibrium was found to be approximately 2 to 3 hours at 2,000 rpm. In the six cores studied, no change in fluid saturation was observed after three hours of centrifuging. This was due to the high permeabilities of the samples.

The capillary pressure is 0 psi at the outer end of the core (i.e. where 100 per cent water saturation is assumed to exist) and it increases with the height to a maximum at the inner end of the core (h = H). The maximum capillary pressure at the inner end of the core (one and a half inches in length) is approximately 6.5 psi. The typical deviation in the average water saturation obtained was 3 percent while the deviation for pressure was 0.2 to 0.3 psi.

Table V - 4 gives a summary of the water volume determinations for the cores. The total volume of water expelled from each core at the end of centrifuging and the water volume extracted from each after centrifuging are
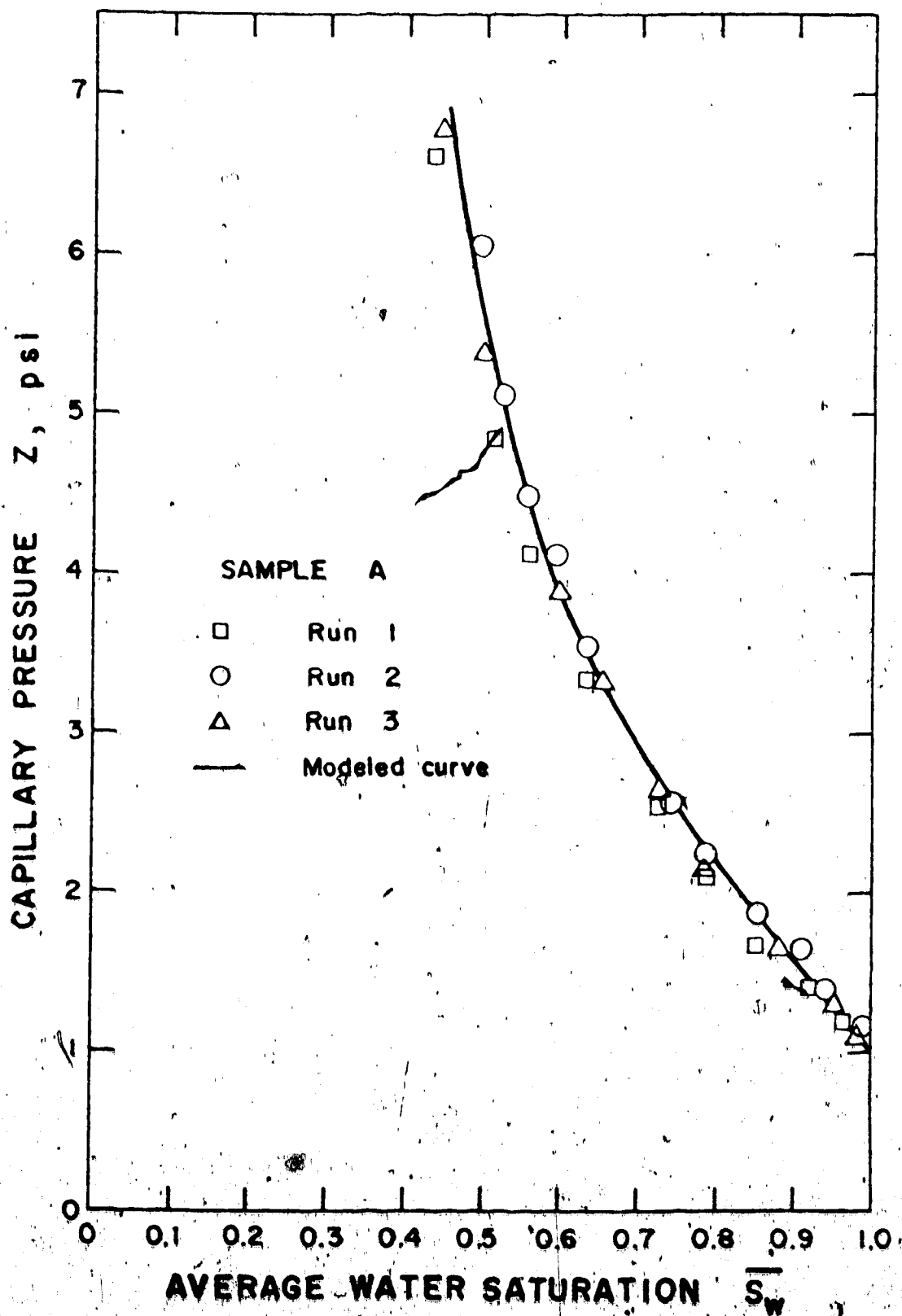
Figure V - 5

Centrifuge Data and the Modeled Curve
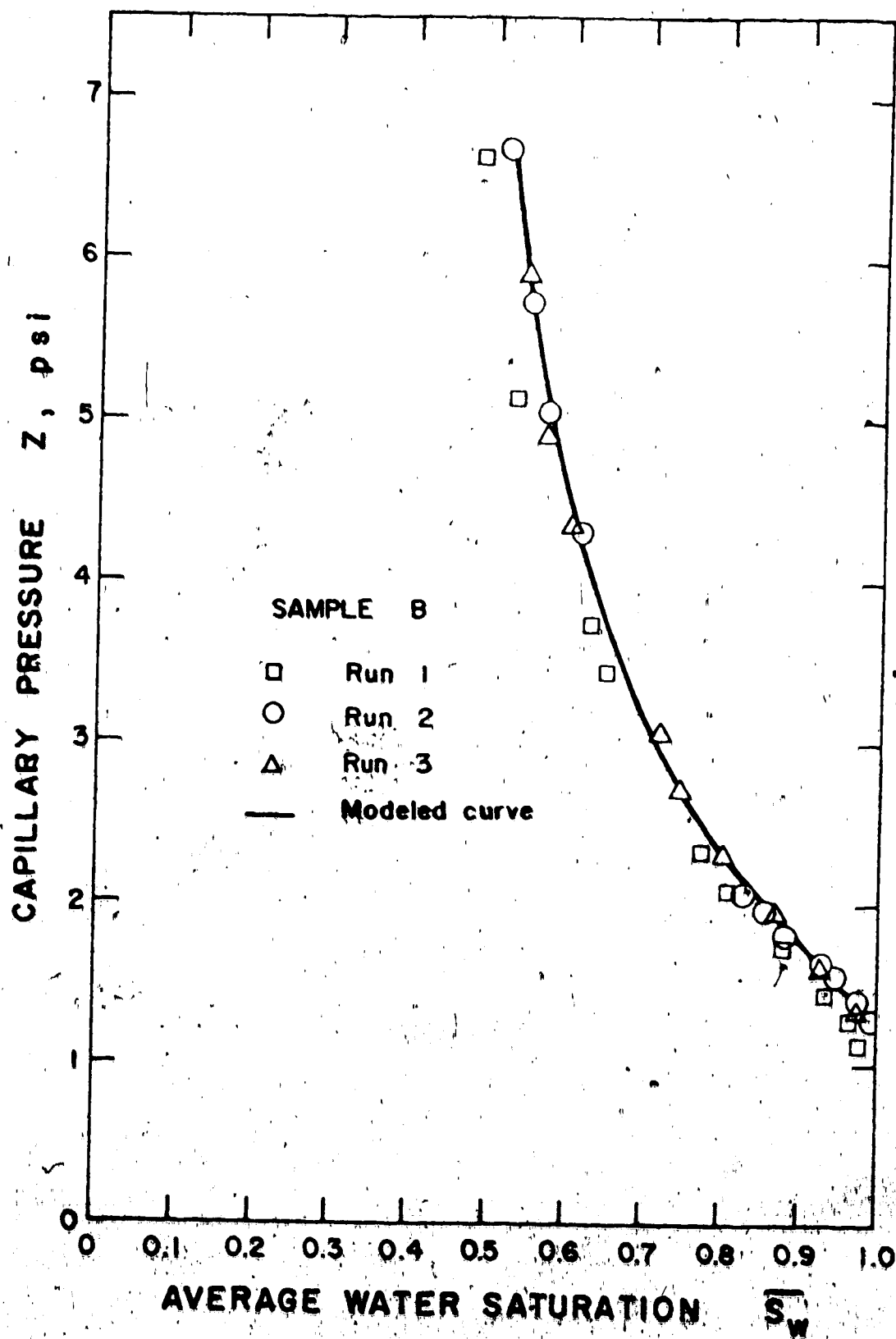
Figure V – 6

Centrifuge Data and the Modeled Curve
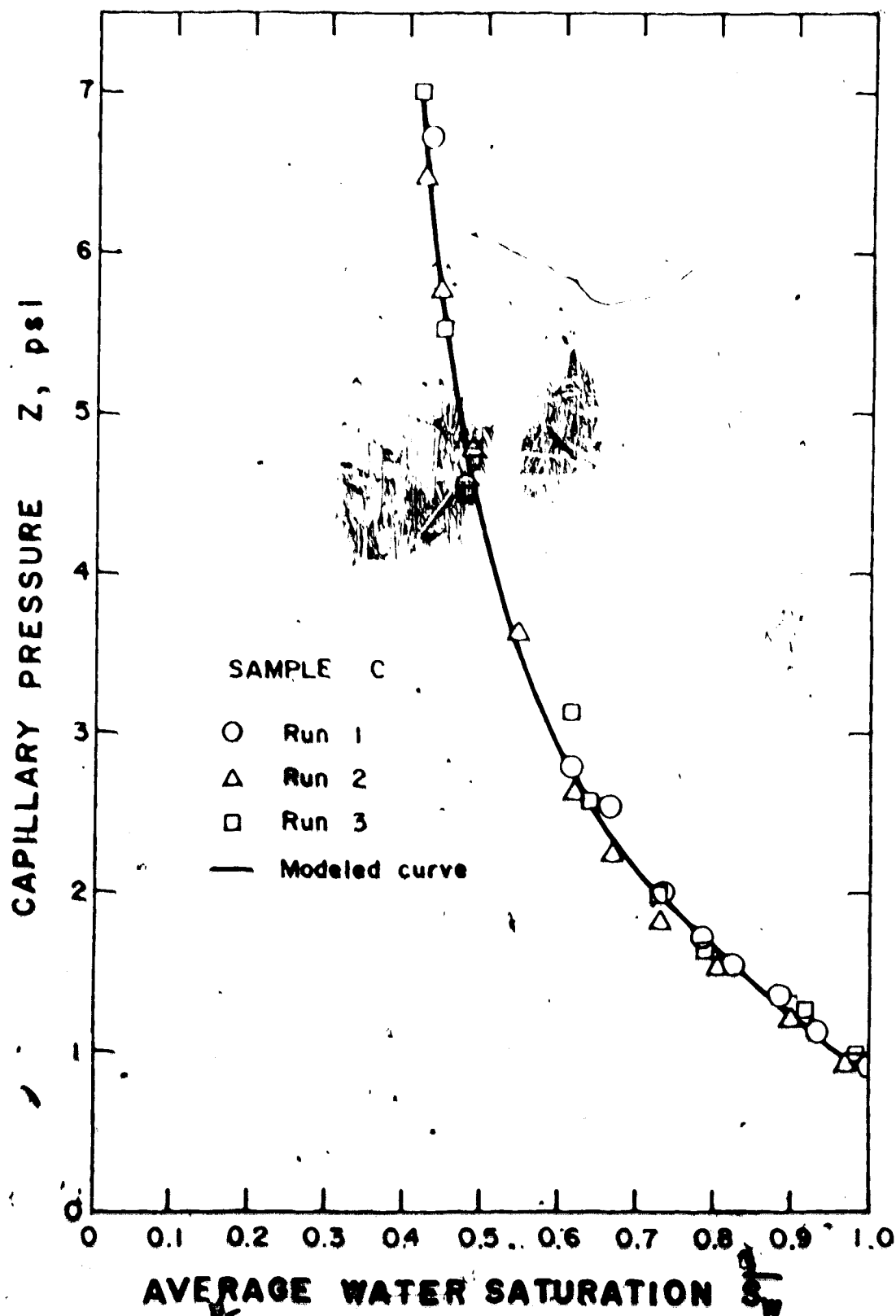
Figure V - 7

Centrifuge Data and the Modeled Curve
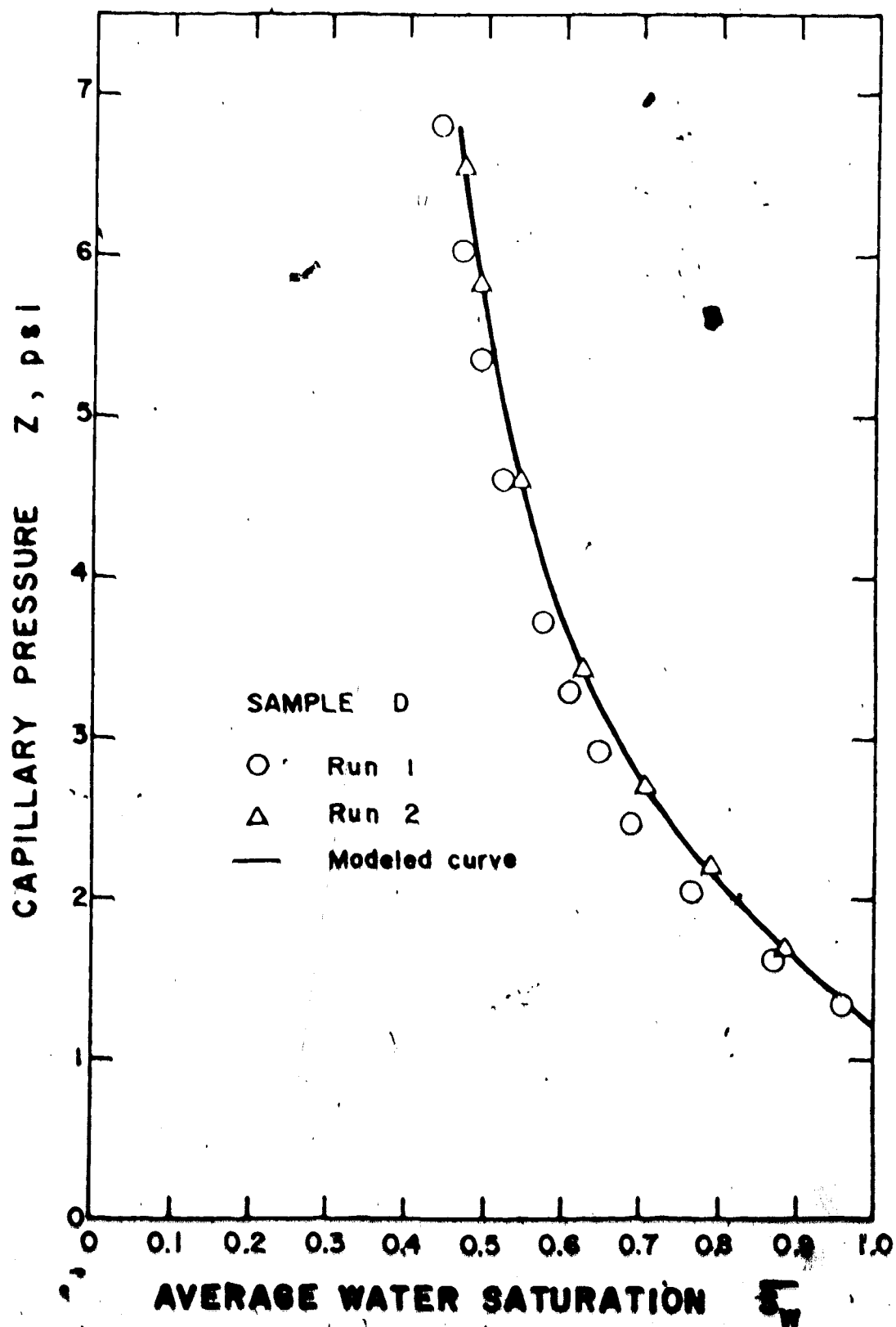
Figure V - 8

Centrifuge Data and the Modeled Curve
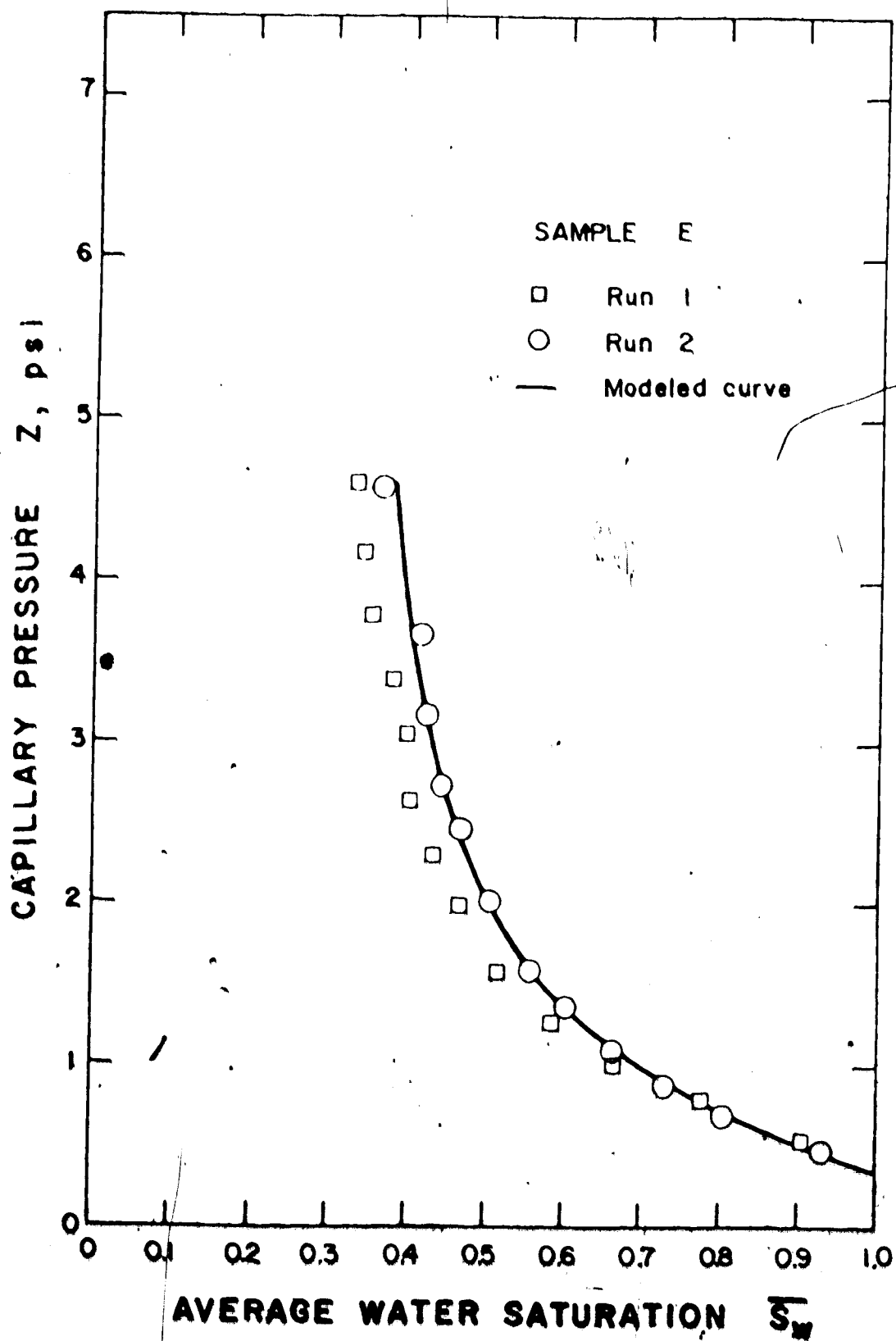
Figure V - 9

Centrifuge Data and the Modeled Curve
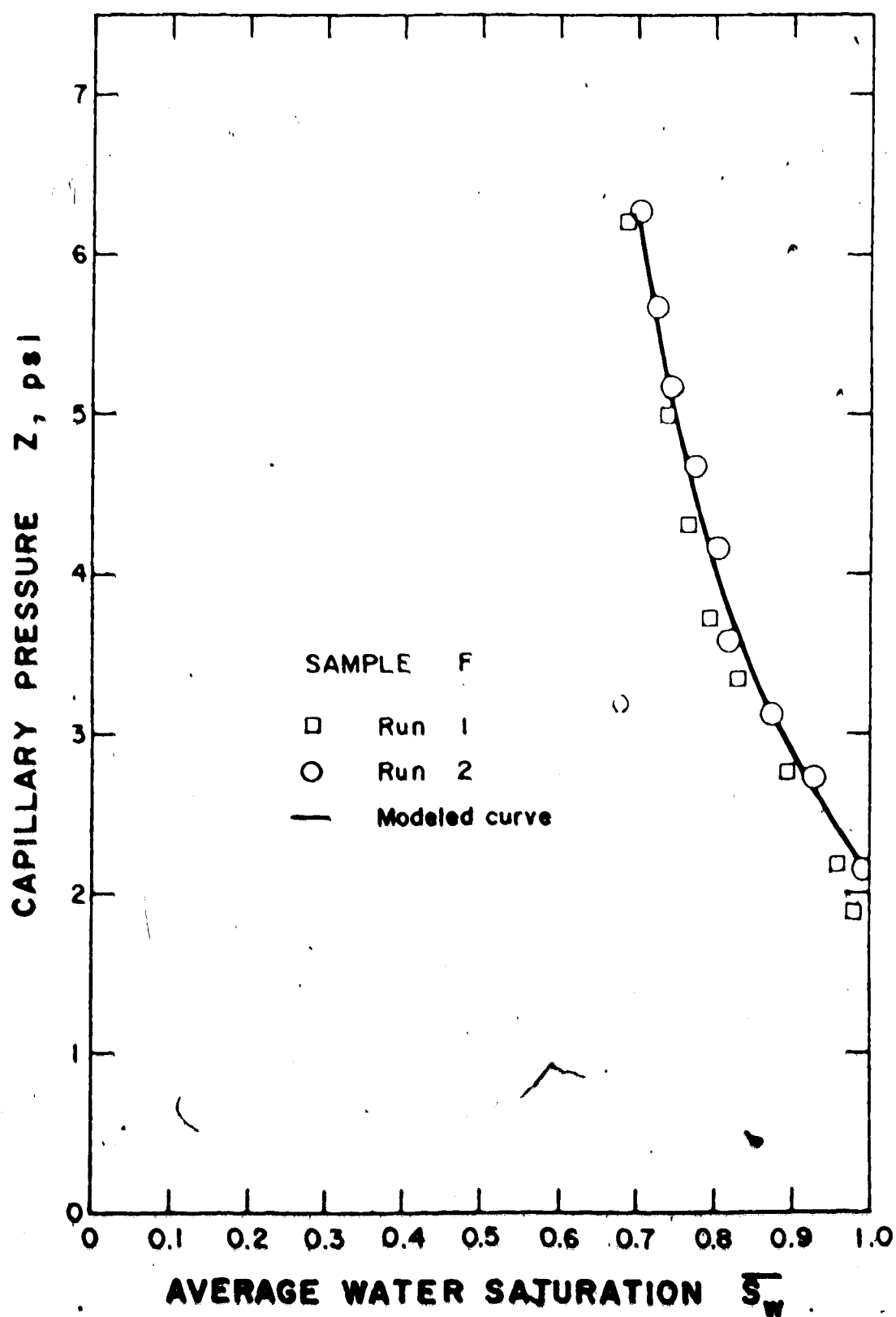
Figure V - 10

Centrifuge Data and the Modeled Curve

TABLE V - 4

WATER VOLUME DETERMINATION

Sample	Run	Water Volume (cc) Displaced (1)	Extracted (2)	Pore Volume (cc) (3)	Error (cc) (3)-(1)-(2)
A	1	2.200	1.65	3.876	0.03
	2	1.956	1.90		0.02
	3	2.160	1.70		0.02
B	1	2.090	1.90	4.030	0.04
	2	2.131	1.85		0.05
	3	1.849	2.15		0.03
C	1	2.445	1.80	4.287	0.04
	2	2.484	1.75		0.05
	3	2.495	1.79		0.09
D	1	1.969	1.50	3.523	0.05
	2	1.862	1.60		0.06
E	1	1.631	0.75	2.439	0.06
	2	1.552	0.82		0.07
F	1	0.845	1.81	2.704	0.05
	2	0.802	1.83		0.06

compared with the pore volume. The error ranges between 0.02 and 0.09 cc. This error is equivalent to 0.5 to 2.3 percent saturation for a typical core.

2. Numerical Results

(i) Modeled Capillary Pressure Curve

The Marquardt Algorithm was employed to obtain S_w versus P_c curve from the experimental data. Two methods were used to apply the model as was mentioned in Chapter III - C.

(1) Numerical Integration Method

The Marquardt Algorithm was used in conjunction with a Gaussian Quadrature 40-point routine to integrate the second term of Equation III - 11.

(2) Approximation Method

The Marquardt Algorithm was applied directly to Equation III - 12.

The parameters of the capillary pressure model were estimated with a convergence criterion of $\varepsilon = 10^{-5}$. Both Numerical Integration and Approximation Methods were used for samples A, B, and C while only the Approximation Method was used for the other samples. The parameter values obtained, their linear confidence limits, and the standard error of estimate are summarized in Table V - 5 and the smoothed values for $\overline{S_w}$ are given in Tables D - 1 through D - 6 in Appendix D. Generated capillary pressure curves are shown

TABLE V - 5

PARAMETER VALUES AND THE STANDARD ERROR OF ESTIMATE

Sample		S_{wi} $\pm$ linear	Parameters confidence limits σ	P_d	Standard Error of Estimate $\times 10^{-2}$
A	Num.	0.268 ± 0.037	1.024 ± 0.217	0.894 ± 0.072	1.062
	App.	0.260 ± 0.038	0.991 ± 0.211	0.901 ± 0.071	1.053
B	Num.	0.369 ± 0.018	0.654 ± 0.123	1.090 ± 0.054	0.747
	App.	0.364 ± 0.019	0.632 ± 0.125	1.096 ± 0.053	0.734
C	Num.	0.300 ± 0.022	0.547 ± 0.130	0.776 ± 0.067	1.537
	App.	0.295 ± 0.023	0.523 ± 0.127	0.782 ± 0.067	1.527
D		0.296 ± 0.015	0.681 ± 0.116	1.031 ± 0.064	0.368
E		0.285 ± 0.019	0.349 ± 0.075	0.282 ± 0.029	0.936
F		0.557 ± 0.031	0.291 ± 0.367	2.019 ± 0.282	0.967

graphically in Figures V - 11 and V - 12, where the single curves seen are sufficient to describe both methods.

(ii)   A Modified Hassler Method

The capillary pressure curve for sample D, run 2, was obtained by applying a modified Hassler method, for which the Spline Fit Technique[25] was used. In this technique, data points are arbitarily divided into several intervals, and the points in each interval are smoothed with a cubic polynomial, making the first two derivatives of the curve on the right-hand side of a boundary point equal to the first two derivatives of the curve on the left-hand side of the boundary point evaluated at the boundary point. The differentiation of the resulting cubic polynomial gives $d(Z\overline{S_w})/dZ$, thus avoiding Hassler's tedious graphical differentiation.

The results obtained using the modified Hassler method is given in Table D - 7 in Appendix D. The solid line in Figure V - 13 represents the results obtained by the Approximation Method while the circles represent the saturation calculated using the modified Hassler scheme. Essentially the same results were obtained using both techniques.

C.   Discussion

1.   Experimental Results

The first runs on samples A and B showed a large deviation from the other two runs. There is some basis for believing that this behavior may have been caused by the unstable wetting properties of the samples at the time of the
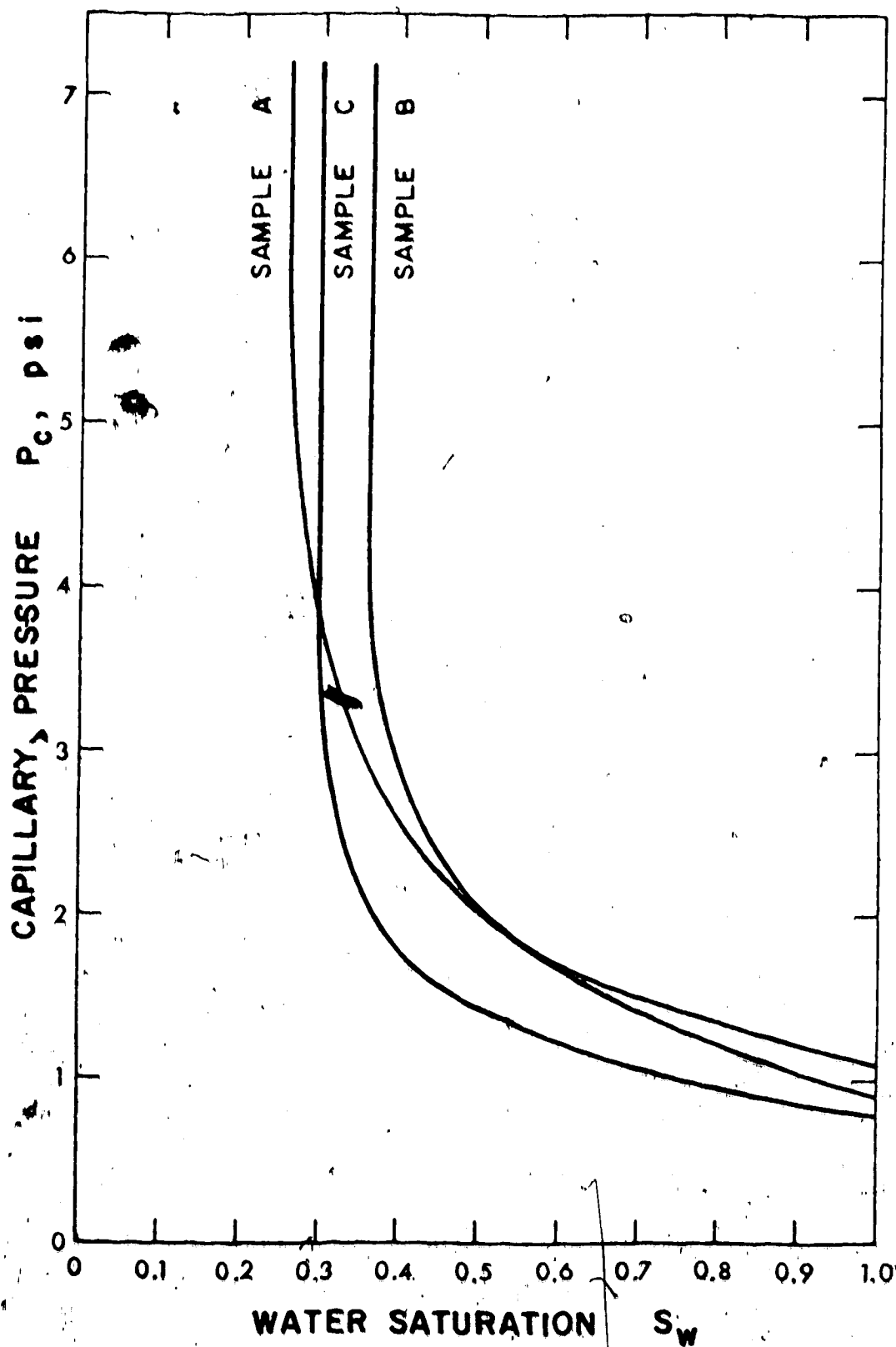
Figure V - 11

Generated Capillary Pressure Curves

CAPILLARY PRESSURE Pc, psi

WATER SATURATION Sw

SAMPLE E

SAMPLE D

SAMPLE F
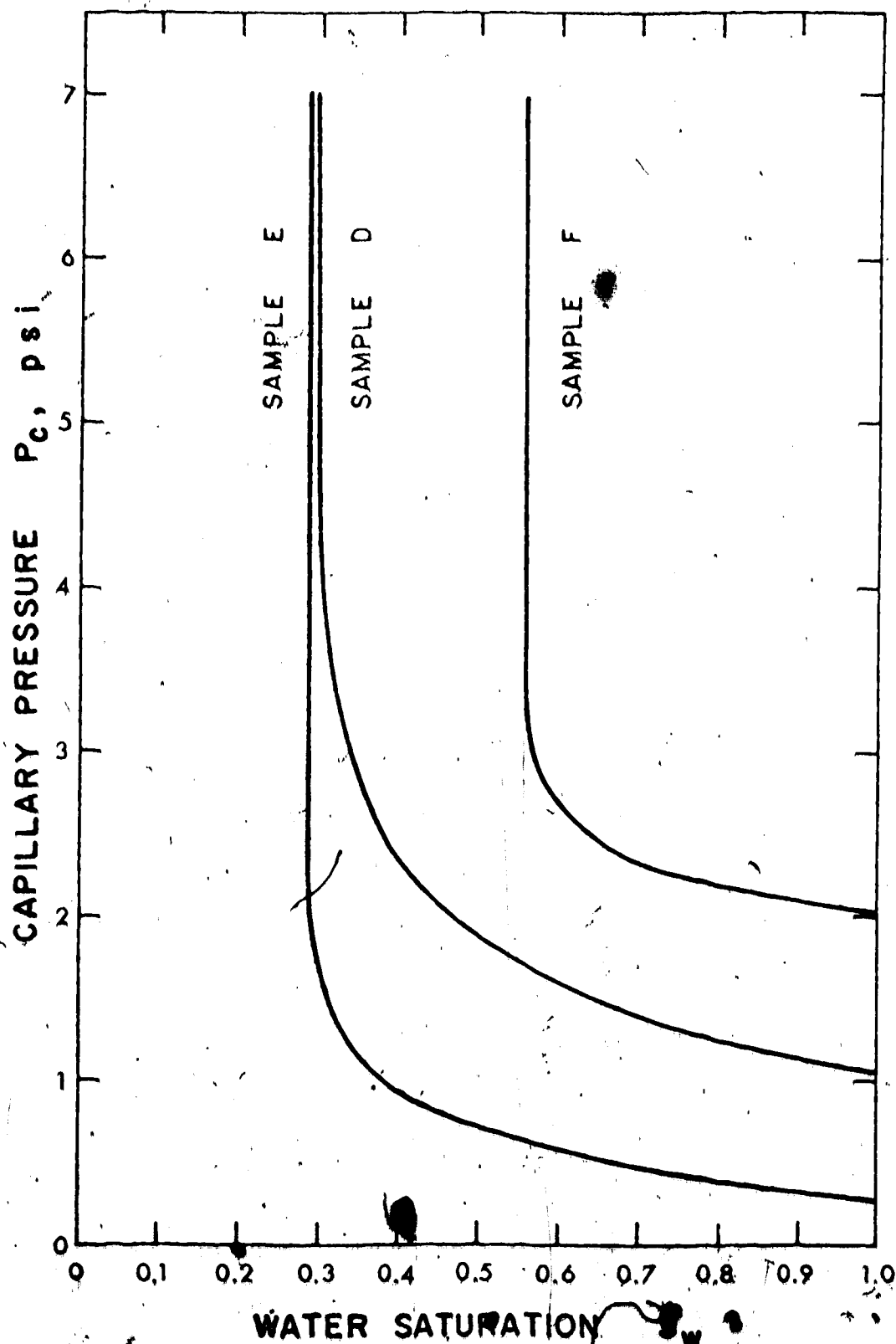
Figure V - 12

Generated Capillary Pressure Curves
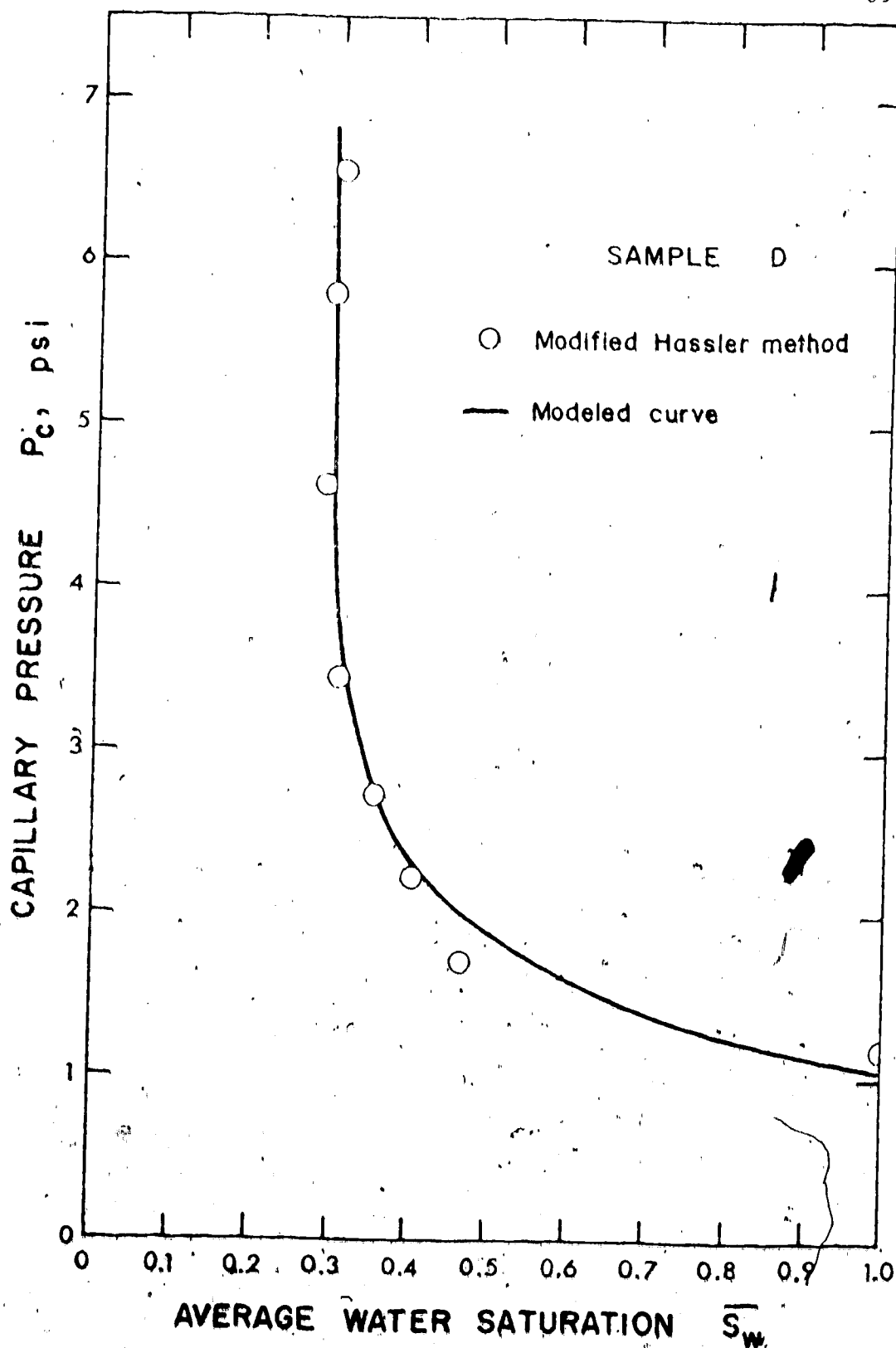
Figure V - 13

Comparison Between Proposed and Hassler's Method

first run.(6)   It is expected that a number of repeated runs
may have eventually stabilized the wettability.   It is for
this reason that the results for the initial runs for all
the samples were not taken into consideration for estimating
parameters of the capillary pressure model except for sample
C whose results for the first run did not show such behavior.

The error involved in the determination of the water
volume in the pipette is estimated to be ± 0.013 cc when the
pipette is magnified 3 times the actual size on photographic
paper.   The uncertainty in saturation would then range
between 0.8 and 2.6 percent.   The typical deviation in the
average saturation (three percent) and the actual error in
water volume determination (Table V - 4) indicates that the
average saturation was determined with satisfactory accuracy.

The stroboscope was calibrated to ± 1% tolerance.
At 2,000 rpm, this is equivalent to 0.13 psi for a typical
sample.   Considering the possibilities of other error sources,
such as very slight centrifuge speed fluctuation, the typical
deviation of pressure (0.2 to 0.3 psi), may be considered to
be small.

Table V - 6 shows the estimated connate and resultant
water saturations for each sample.   The maximum rotation
speed for the centrifuge was 2,200 rpm.   This was insufficient
to drive the water saturation to the connate water saturation.
Thus the resultant water saturations were considerably
greater than the connate water saturations.

TABLE V - 6

RESULTANT AND ESTIMATED CONNATE WATER SATURATIONS

Sample	Resultant Saturation	Connate Water Saturation
A	0.464	0.260
B	0.496	0.363
C	0.408	0.295
D	0.455	0.296
E	0.336	0.285
F	0.763	0.557

2. Numerical Results

(i) Suggested Method Using the Model

Relatively large linear confidence limits are seen for σ in Table V - 5 as compared with S_{wi} and P_d, indicating that σ is sensitive to small changes in capillary pressure data. The phenomenon can possibly be explained by noting that the samples used are not homogeneous. Though the standard errors of estimates ranged between 0.368×10^{-2} and 1.537×10^{-2}, they are considered to be satisfactorily small.

The differences between the parameters obtained in the two methods are much smaller than the linear confidence limits. Good agreement between the two methods leads to the suggestion that due to its simplicity only the Approximation Method need be used.

(ii) Modified Hassler Method and Suggested Method

The modified Hassler method has given essentially the same results as the Approximation Method (See Figure V - 13). Use of numerical differentiation rather than graphical differentiation eases the application of Hassler's theory[19] considerably.

A problem with the Spline Fit Technique is the selection of boundary points. As the cubic polynomial for each interval is dependent on the choice of boundary points, changing boundary points normally results in some change in derivatives also. Apparently, no theoretical

studies have been made as to the optimum choice of boundary points associated with this technique. However, this should not be too serious a problem as long as data points are reasonably smooth.

3. The End Effect

It has long been noted that where there is a discontinuity in the capillary properties at the outflow end of the core sample, capillarity in the core tends to draw the water into the core from the void. The water thus accumulates in the boundary, and the increased water saturation causes a decrease in the permeability to oil.[28] This behavior is called the "end effect" or the "boundary effect".

In the reservoir or large-scale laboratory experiments, the distorted zone caused by the end effect has a relatively small effect on the interpretation of results. However, in a small-scale laboratory experiment, it is very important to account adequately for this effect. Thus, in the membrane method, it is customary to place some porous material saturated with the wetting-fluid between the sample and the semi-permeable membrane to ensure phase continuity and thus eliminate the end effect. In the centrifuge method, however, the end effect has often been ignored despite the absence of an end-butt in most experimental set-ups. The question arises, therefore, if the end effect would violate seriously the assumption made by Hassler that $P_c = 0$ at $h = 0$.

It is clear from Leverett's explanation of the end effect[28] that the pressure in the water must be considerably higher than that in the oil just outside the core, in order that displacement take place. Figures V - 14-A to V - 14-C show the pressure distribution in the oil and water within the core in three different situations. Figure V - 14-A is the distribution on which Hassler's assumption is based. Figure V - 14-B shows the pressure distribution expected when the capillary displacement is taking place, and Figure V - 14-C shows the distribution when the system is in capillary equilibrium. As the oil pressure is greater than the water pressure at the inner end of the core, the capillary pressure inversion must take place somewhere in the core. It is expected that the location of inversion (at which $P_C = 0$) would move toward the outer end of the core as the system approaches capillary equilibrium. The same effect is expected as the centrifugal acceleration increases.

Strictly speaking, however, the location at which $P_C = 0$ would never reach the outer end of the core. Thus the end effect violates Hassler's assumption and may result in higher displacement and capillary pressures until the centrifugal force increases sufficiently to reduce this adverse effect to a negligible level. Furthermore, negative capillary pressure at the outer end of the core indicates the saturation at the location just outside this end face is not 100 percent oil. This would result in higher observed
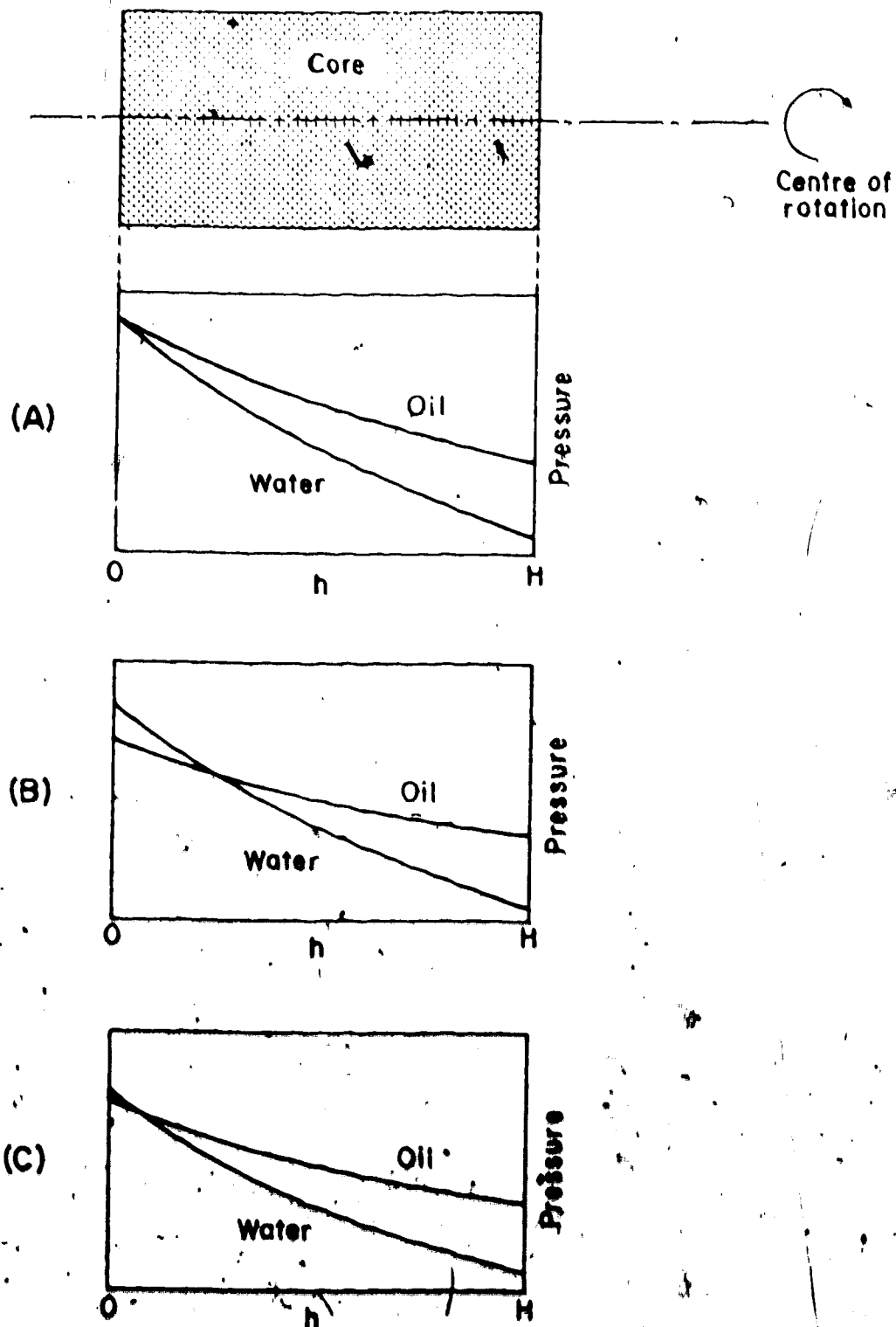
Figure V - 14

Pressure Distributions within a Porous Medium
Being Rotated in a Centrifuge

average saturation. The end effect, however, does not seem to affect Hassler's assumption too seriously, as the more acceleration increases, the more the assumption seems likely to be reasonable. This is further confirmed by the agreement between the membrane and the centrifuge method results reported by Hassler and the centrifuge test done by Marx[31] with and without an end-butt.

At this point, it should be noted that the displacement pressure estimated using the proposed method is considerably lower than the value obtained by extrapolating data plots (Figure V - 5 to V - 10) to $S_w = 1$. In order to interpret the results adequately the discrepancies are tabulated in Table V - 7 and are plotted against permeability in Figure V - 15. It seems from Figure V - 15 that a linear correlation may exist between the discrepancy and permeability; the discrepancy increases with permeability. Laverett[28] explains this tendency by saying that the greater the permeability, the greater the distance over which the appreciable distortion takes place. The anomalous result for sample E can be explained by noting that it is much shorter than other samples.

As to the discrepancies found between the experimentally obtained P_d and the estimated P_d, the following explanation can be made. The Marquardt Algorithm estimates parameters using all data points equally weighted. Therefore, even though the data are slightly in error in the relatively

...

TABLE V - 7

PERMEABILITIES AND THE DISPLACEMENT PRESSURE DISCREPANCIES

Sample	K (md)	$P_{d_{est.}}$ (psi)	$P_{d_{exp.}}$ (psi)	Discrepancy (percent) $\frac{(2)-(1)}{(2)} \times 100$
A	253	0.901	1.030	12.5
B	255	1.096	1.239	11.5
C	429	0.782	0.912	14.2
D	146	1.031	1.155	10.1
E	400	0.282	0.397	28.9
F	30	2.019	2.046	1.3
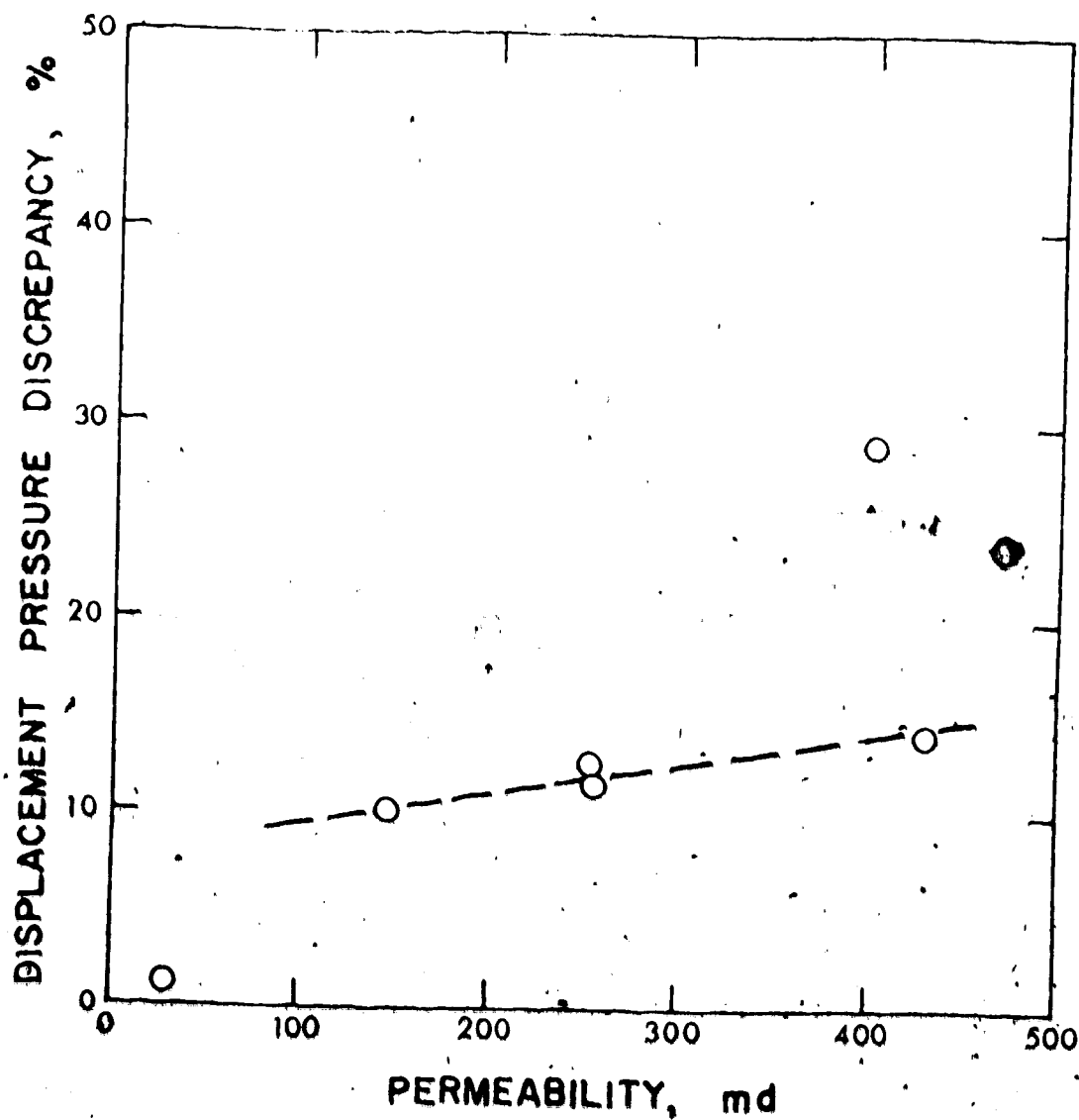
Figure V - 15

Displacement Pressure Discrepancies
and Permeabilities

low pressure region, the model would estimate a P_d which would likely be closer to the true P_d than that obtained by extrapolation. As the P_d obtained by extrapolation is expected to be higher than the true P_d, the lower P_d estimated using the model may thus be justified. It should be noted however, that the deviation of the estimated P_d from that observed is not necessarily a quantitative representation of the end effect, but could also be a result of the heterogeneity of the sample.

CHAPTER VI

CONCLUSIONS AND RECOMMENDATIONS

1. Conclusions

As a result of this investigation, the following conclusions can be made:

(1) A drainage capillary pressure model has been suggested in this study. The model describes the capillary pressure-saturation relationship in a porous medium satisfactorily.

(2) The model has been experimentally verified using data obtained from relatively homogeneous, water-wet, sandstone cores, and using several different fluid combinations. This limited amount of experimental data suggests that the correlation may be universal.

(3) The model can readily be applied to the data obtained using a centrifuge. Numerical Integration and Approximation Methods were used. Due to the good agreement, the Approximation Method is recommended for practical use because of its simplicity.

(4) Good agreement was found between the Approximation Method and the conventional (Hassler) method.

(5) The application of the model to the centrifuge data has the following advantages over the conventional method:

    (i)   Data can be smoothed, the connate water

saturation and the displacement pressure

estimated, and the capillary pressure curve

generated readily and efficiently.

    (ii)   Tedious graphical or numerical differentiation

at the data points is unnecessary.

(6) The model estimates a lower displacement pressure

than that observed. The estimated displacement

pressure is probably closer to the true value.

(7) Data obtained using the membrane method (P_g versus S_w)

can be regarded as P_c versus S_w provided the core is

sufficiently short.

2.   <u>Recommendations</u>

(1) To further investigate the validity of this model:

    (i)   The membrane method should be used in conjunc-

tion with the centrifuge method applied here.

    (ii) Homogeneous samples should be studied.

    (iii) The end effect should be further investigated.

(2) Regarding this experiment:

    (i)   To further reduce the systematic error inherent,

a refrigerated type of centrifuge is desirable.

The importance of the accuracy of the speed

control can not be over-emphasized.

    (ii) Photographic determination of the fluid volume

displaced was efficient and accurate; however,

the stroboscope and the centrifuge speed should

be electronically synchronized.

(iii) To investigate the capillary pressure of

samples over a broader range of permeability

and porosity would require a higher speed

centrifuge.

(3) Experimental runs should be repeated a sufficient

number of times on the same sample to stabilize

wettability.

NOMENCLATURE

NOMENCLATURE

At   adhesion tension, $ergs/cm^2$

g   force of gravity, cm/sec^2

H   height of sample, cm

h   height from the outer end of a core to any location in the core, cm

K   permeability, Darcies

L   length, cm

n   rotation speed, rpm

P   pressure, psi

R   distance from the centre of rotation to the outer end of a core

S   saturation, fraction

Z   the capillary pressure at the inner end of a core in the centrifuge, psi

a centrifugal acceleration, cm/sec^2

γ interfacial tension, dynes/cm

θ contact angle

ρ density, gm/cm^3

σ capillary pressure normalizing parameter, psi

ϕ porosity, fraction

ω angular velocity, radians/sec

π normalized pressure, dimensionless

Subscripts

c   capillary or critical

d   displacement

g   gas

i   initial

o   oil

r   residual

s   solid

w   water

BIBLIOGRAPHY

BIBLIOGRAPHY

(1) Amott, E.: "Observations Relating to the Wettability of Porous Rock," Trans. AIME (1959) Vol. 216, pp. 156-162.

(2) Amyx, J. W., Bass, D. M. Jr., and Whiting, R. L.: Petroleum Reservoir Engineering--Physical Properties, McGraw Hill, New York, 1960.

(3) Bartell, F. E., and Osterhof, H. J.: "Determination of the Wettability of a Solid by a Liquid," Ind. Eng. Chem. (Nov., 1927) Vol. 19 (11), pp. 1277-1280.

(4) Benner, F. C., and Bartell, F. E.: "The Effect of Polar Impurities upon Capillary and Surface Phenomena in Petroleum Production," Drill. and Prod. Prac., API (1941), pp. 341-345.

(5) Bobek, J. E., Mattax, C. C., and Denekas, M. O.: "Reservoir Rock Wettability--Its Significance and Evaluation," Trans. AIME (1958) Vol. 213, pp. 155-160.

(6) Brigham, W.: Personal Communication.

(7) Brown, H. W.: "Capillary Pressure Investigations," Trans. AIME (1951) Vol. 192, pp. 67-74.

(8) Brownscombe, E. R., et al.: "Laboratory Determination of Relative Permeability," Oil and Gas J. (Feb., 1950) Vol. 48. (41), pp. 98-102, 123.

(9) Bruce, W. A., and Welge, H. J.: "The Restored State Method for Determination of Oil in Place and Connate Water," Drill. and Prod. Prac., API (1947) 166-174.

(10) Calhoun, J. C. Jr.: Fundamentals of Reservoir Engineering, Univ. of Oklahoma Press, Norman, 1953.

(11) Calhoun, J. C., Jr., Lewis, M., Jr., and Newman, R. C.: "Experiments on the Capillary Properties of Porous Solids," Trans. AIME (1949) Vol. 186, pp. 189-196.

(12) Coley, F. H., Marsden, S. S., and Calhoun, J. C.: "A Study of the Effect of Wettability on the Behavior of Fluids in Synthetic Porous Media," Prod. Monthly (June, 1956), pp. 29-45.

(13) Craig, F. F., Jr.: The Reservoir Engineering Aspects of Waterflooding, Monograph Vol. 3, Soc. Pet. Eng. of AIME, 1971.

(14) Donaldson, E. C., Thomas, R. D., and Lorentz, P. B: "Wettability Determination and Its Effect on Recovery Efficiency," Soc. Pet. Eng. J. (Mar., 1969), pp. 13-20.

(15) Dumore, J. M., and Schlos, R. S.: "Drainage Capillary-Pressure Functions and Their Computation from One Another," SPE 4096, Preprint for the 47th Annual Fall Meeting of the Society of Petroleum Engineers of AIME, Tex., (Oct., 8-10), 1972.

(16) Fayers, F. J., and Sheldon, J. W.: "The Effects of Capillary Pressure and Gravity on Two-Phase Fluid Flow in a Porous Medium," Trans. AIME (1959) Vol. 216, pp. 147-155.

(17) Gatenby, W. A., and Marsden, S. S.: "Some Wettability Characteristics of Synthetic Porous Media," Prod. Monthly (Nov., 1957) Vol. 22, pp. 5-12.

(18) Hassler, G. L.: "Method and Apparatus for Permeability Measurement," U.S. Patent No. 2345935 (Ap., 1944).

(19) Hassler, G. L., and Brunner, E.: "Measurement of Capillary Pressure in Small Core Samples," Trans. AIME (1945) Vol. 160, pp. 114-123.

(20) Hassler, G. L., Brunner, E., and Deahl, T. J.: "The Role of Capillarity in Oil Production," Trans. AIME (1944) Vol. 155, pp. 155-174.

(21) Henderson, J. H., and Yuster, S. T.: "Relative Permeability Studies," Prod. Monthly (1947) Vol. 12, p. 13.

(22) Hoffman, R. N.: "A Technique for the Determination of Capillary Pressure Curves Using a Constantly Accelerated Centrifuge," Soc. Pet. Eng. J. (Sept., 1963), pp. 227-235.

(23) Jennings, H. Y., Jr.: "Surface Properties of Natural and Synthetic Porous Media," Prod. Monthly (Mar., 1957), pp. 20-24.

(24) Kinney, P. T., and Nielsen, R. F.: "The Role of Wettability in Oil Recovery," Prod. Monthly (Jan., 1950), pp. 29-35.

(25) Klaus, R. L., and Van Ness, H. C.: "An Extension of the Spline Fit Technique and Applications to Thermodynamic Data," AIChE J. (Nov., 1967), pp. 1132-1136.

(26) Kyte, J. R.: "A Centrifuge Method to Predict Matrix-Block Recovery in Fractured Reservoirs," Soc. Pet. Eng. J. (June, 1970), pp. 164-170.

(27) Leas, W. J., Jenks, L. H., and Russell, C. D.: "Relative Permeability to Gas," Trans. AIME (1950) Vol. 189, pp. 65-72.

(28) Leverett, M. C.: "Capillary Behavior in Porous Solids," Trans. AIME (1941) Vol. 142, pp. 152-169.

(29) Levorsen, A. I.: Geology of Petroleum, W. H. Freeman and Co., San Francisco, 1954.

(30) Marquardt, D. W.: "An Algorithm for Least-Squares Estimation of Nonlinear Parameters," J. Soc. Indus. Appl. Math. (1963) Vol. 11 (2), pp. 431-441.

(31) Marx, J.,W.: "Determining Gravity Drainage Characteristics on the Centrifuge," Trans. AIME (1956) Vol. 207, pp. 88-91.

(32) McCardell, W. M.: "A Review of the Physical Basis for the Use of the J-function," Eighth Oil Recovery Conference, Texas Petroleum Research Committee, 1955.

(33) McCullough, J. J., Albaugh, F. W., and Jones, P. H.: "Determination of the Interstitial-Water Content of Oil and Gas Sand by Laboratory Tests of Core Samples," Drill. Prod. Prac., API (1944), pp. 180-188.

(34) Morrow, N. R.: "The Retention of Connate Water in Hydrocarbon Reservoir. Part I. A Review of Basic Principles," J. Canadian Petroleum (1971) Vol. 10 (1), pp. 38-46.

(35) Morrow, N. R.: "The Retention of Connate Water in Hydrocarbon Reservoir. Part II. Environment and Properties of Connate Water," J. Canadian Petroleum (1971) Vol. 10 (1), pp. 47-55.

(36) Mungan, N.: "Role of Wettability and Interfacial Tension in Water Flooding," Soc. Pet. Eng. J. (June, 1961), pp. 115-123.

(37) Newcombe, J., McGhee, J., and Rzasa, M. J.: "Wettability versus Displacement in Water Flooding in Unconsolidated Sand Columns," Trans. AIME (1955) Vol. 204, pp. 227-232.

(38) Pickell, J. J., Swanson, B. F., and Hickman, W. B.: "Application of Air-Mercury and Oil-Air Capillary Pressure Data in the Study of Pore Structure and Fluid Distribution," Soc. Pet. Eng. J. (Mar., 1966), pp. 55-61.

(39) Plateau, J. A. F.: "Experimental and Theoretical Research on the Figures of Equilibrium of a Liquid Mass Withdrawn from the Action of Gravity," Smith Inst. Ann. Repts., pp. 1863-1866.

(40) Purcell, W. R.: "Capillary Pressure--Their Measurements Using Mercury and the Calculation of Permeability Theorum," Trans. AIME (1947) Vol. 186, pp. 39-48.

(41) Ritter, H. L., and Drake, L. C.: "Pore-Size Distribution in Porous Materials," Ind. Eng. Chem., Ann. Ed. (1945) Vol. 17, pp. 782-786.

(42) Ritter, H. L., and Drake, L. C.: "Macropore-Size Distribution in Some Typical Porous Substances," Ind. Eng. Chem., Ann. Ed. (1945) Vol. 17, pp. 786-791.

(43) Rose, W., and Bruce, W. A.: "Evaluation of Capillary Character in Petroleum Reservoir Rock," Trans. AIME (May, 1949) Vol. 186, pp. 127-142.

(44) Scott, J. D.: Controlled Chemical Waterflooding of Viscous Crude Oil, M. Sc. Thesis in Petroleum Engineering, Univ. of Alberta, 1971.

(45) Slobod, R. L., and Blum, H. A.: "Method for Determining Wettability of Reservoir Rocks," Trans. AIME (1952) Vol. 195, pp. 1-4.

(46) Slobod, R. L., and Chambers, A.: "Use of Centrifuge for Determining Connate Water, Residual Oil and Capillary Pressure Curves of Small Core Samples," Trans. AIME (1951) Vol. 192, pp. 127-134.

(47) Szabo, M. T.: "New Method for Measuring the Imbibition Capillary Pressure and Electrical Resistivity Curves by Centrifuge," 45th Ann. Fall Mtg., Soc. Pet. Eng., Houston, Tex., (Oct., 4-7), 1970.

(48) Szabo, M. T.: "The Role of Gravity in Capillary Pressure
     Measurements," Soc. Pet. Eng. J. (Ap., 1972), pp.
     85-88.

(49) Thornton, O. F., and Marshall, D. L.: "Estimating
     Interstitial Water by the Capillary Pressure Method,"
     Trans. AIME (1947) Vol. 186, pp. 69-80,

(50) Wagner, O. R., and Leach, R. O.: "Improving Oil Displace-
     ment Efficiency by Wettability Adjustment," Trans.
     AIME (1959) Vol. 216, pp. 65-72.

(51) Welge, H. J.: "Displacement of Oil from Porous Media by
     Water or Gas," Trans. AIME (1949) Vol. 179, pp.
     133-145.

(52) Wenzel, R. N.: "Resistance of Solid Surfaces to Wetting
     by Water," Ind. Eng. Chem. (1935) Vol. 28 (8), pp.
     988-991.

APPENDICES

APPENDIX A

DERIVATION OF EQUATION III - 10

APPENDIX A

Given:

$$P_c = \Delta\rho\omega^2 (R - \frac{h}{2})h \qquad (A - 1)$$

$$\omega_c = \sqrt{\frac{P_d}{\Delta\rho (R' - \frac{H}{2})H}} \qquad (A - 2)$$

and

$$h^* = R - \sqrt{R^2 - \frac{2P_d}{\Delta\rho\omega^2}} \qquad (A - 3)$$

By definition

$$\overline{S_w} = \frac{1}{H}\left[\int_0^H S_{wi} + (1 - S_{wi}) \exp(-\frac{P_c - P_d}{\sigma}) dh \right]$$

$$(A - 4)$$

But

$$S_w = 1 \text{ for } P_c \leq P_d$$

Then

$$\overline{S_w} = \frac{1}{H}\left[\int_0^{h^*} dh + \int_{h^*}^H S_{wi} + (1 - S_{wi}) \exp(-\frac{P_c - P_d}{\sigma}) dh \right]$$

$$(A - 5)$$

where h^* is the location within a core at which $P_c = P_d$.
From Equation A - 1,

$$dh = \frac{dP_c}{\Delta\rho\omega^2 \sqrt{R^2 - \frac{2P_c}{\nabla\rho\omega^2}}} \qquad (A - 6)$$

By substituting the variable h with P_c and defining

$$Z = \Delta\rho\omega^2 (R - H/2) H \qquad (A - 7)$$

the following equation will result:

$$\overline{S_w} = S_{wi} + \frac{(1 - S_{wi})h^*}{H} + \frac{(1 - S_{wi})}{\Delta\rho\omega^2 H}$$

$$x \int_{P_d}^{Z} \frac{\exp(-\frac{P_c - P_d}{d})}{\sqrt{R^2 - \frac{P_c(2R - H)H}{Z}}} dP_c \qquad (A - 8)$$

APPENDIX. B

DERIVATION OF EQUATIONS V - 1 AND V - 2

APPENDIX B

For $P_c \geq P_d$,

$$S_w = S_{wi} + (1-S_{wi}) \exp \left(- \frac{P_c - P_d}{\sigma}\right) \qquad (B - 1)$$

But, the capillary pressure within a core in the membrane method varies with height due to gravity. Define

$$P_c = P_g + \rho_w g h \qquad (B - 2)$$

and

$$Z = P_g + \rho_w g H \qquad (B - 3)$$

Case 1: $P_g \leq P_d \leq Z$

$$P_d = P_g + \rho_w g h* \qquad (B - 4)$$

where h* is the location within a core at which $P_c = P_d$,

$$\overline{S_w} = \frac{1}{H} \left[\int_0^{h*} dh + \int_{h*}^{H} S_{wi} + (1-S_{wi}) \exp\left(- \frac{P_c - P_d}{\sigma}\right) dh \right]$$

$$= S_{wi} + \frac{(1-S_{wi})}{H} \left[h* + \int_{h*}^{H} \exp\left(- \frac{P_c - P_d}{\sigma}\right) dh \right] \qquad (B - 5)$$

From Equation B - 2

$$dh = \frac{dP_c}{\rho_w g}$$

96

By substituting the variable h with P_C and h^* with $(P_d - P_g)/\rho_w g$, the following equation will result:

$$\overline{S_w} = S_{wi} + \frac{(1 - S_{wi})}{\rho_w gH}\left[P_g - P_d + \sigma\left\{1 - \exp\left(-\frac{Z - P_d}{\sigma}\right)\right\}\right]$$

(B - 7)

Case 2: $\quad P_g \geq P_d$

$$\overline{S_w} = \frac{1}{H}\int_0^H S_{wi} + (1 - S_{wi})\exp\left(-\frac{P_C - P_d}{\sigma}\right)dh$$

$$= S_{wi} + \frac{1 - S_{wi}}{H}\int_{P_g}^Z \exp\left(-\frac{P_C - P_d}{\sigma}\right)\frac{dP_C}{\rho_w g}$$

$$= S_{wi} + \frac{\sigma(1 - S_{wi})}{\rho_w gH}\left[\exp\left(-\frac{P_g - P_d}{\sigma}\right) - \exp\left(-\frac{Z - P_d}{\sigma}\right)\right]$$

(B - 8)

Case 3: $\quad P_g = P_d$

$$\overline{S_w} = S_{wi} + \frac{\sigma(1 - S_{wi})}{\rho_w hH}\left[1 - \exp\left(-\frac{Z - P_d}{\sigma}\right)\right] \qquad (B - 9)$$

APPENDIX C

EXPERIMENTAL DATA

TABLE C - 1 - 1

EXPERIMENTAL DATA

SAMPLE A, RUN 1

Centrifuge Speed n rpm	Capillary Pressure Z psi	Average Saturation $\overline{S_W}$
479	0.379	1.000
535	0.473	1.000
685	0.775	1.000
762	0.959	1.000
808	1.078	0.971
848	1.187	0.962
920	1.397	0.918
1006	1.671	0.849
1124	2.086	0.787
1238	2.530	0.726
1424	3.338	0.632
1580	4.121	0.559
1710	4.827	0.514
2000	6.603	0.432

TABLE C - 1 - 2

EXPERIMENTAL DATA

SAMPLE A, RUN 2

Centrifuge Speed n rpm	Capillary Pressure z psi	Average Saturation $\overline{S}_w$
395	0.258	1.000
566	0.529	1.000
685	0.775	1.000
835	1.151	0.990
920	1.397	0.942
1000	1.651	0.911
1065	1.872	0.855
1165	2.240	0.787
1245	2.559	0.745
1465	3.543	0.634
1580	4.121	0.593
1650	4.494	0.558
1760	5.113	0.525
1915	6.054	0.495

TABLE C - 1 - 3

EXPERIMENTAL DATA

SAMPLE A, RUN 3

Centrifuge Speed n rpm	Capillary Pressure z psi	Average Saturation $\overline{S_w}$
476	0.374	1.000
648	0.693	1.000
815	1.096	0.982
890	1.308	0.952
1000	1.651	0.880
1140	2.145	0.783
1265	2.642	0.726
1420	3.329	0.655
1535	3.889	0.598
1805	5.378	0.499
2025	6.769	0.443

TABLE C – 2 –1

EXPERIMENTAL DATA

SAMPLE B, RUN 1

Centrifuge Speed n rpm	Capillary Pressure Z psi	Average Saturation $\overline{S}_w$
421	0.294	1.000
504	0.421	1.000
617	0.631	1.000
700	0.812	1.000
750	0.932	1.000
824	1.125	0.976
880	1.283	0.961
930	1.433	0.933
1020	1.723	0.879
1120	2.078	0.807
1184	2.322	0.774
1440	3.435	0.648
1500	3.727	0.629
1760	5.131	0.529
2000	6.625	0.481

TABLE C - 2 - 2

EXPERIMENTAL DATA

SAMPLE B, RUN 2

Centrifuge Speed n rpm	Capillary Pressure Z psi	Average Saturation $\overline{S_w}$
522	0.451	1.000
620	0.637	1.000
720	0.859	1.000
800	1.060	1.000
878	1.277	0.995
920	1.402	0.975
970	1.558	0.945
996	1.643	0.927
1044	1.805	0.880
1090	1.968	0.856
1120	2.078	0.828
1612	4.304	0.614
1746	5.049	0.569
1860	5.730	0.545
2010	6.692	0.514

TABLE C - 2 - 3

EXPERIMENTAL DATA

SAMPLE B, RUN 3

Centrifuge Speed n rpm	Capillary Pressure z psi	Average Saturation $\overline{S}_w$
485	0.390	1.000
602	0.600	1.000
700	0.812	1.000
765	0.965	1.000
840	1.169	1.000
900	1.342	0.975
985	1.607	0.929
1085	1.950	0.867
1180	2.306	0.804
1280	2.714	0.746
1360	3.064	0.719
1620	4.347	0.605
1720	4.900	0.568
1890	5.916	0.541

TABLE C - 3 - 1

EXPERIMENTAL DATA

SAMPLE C, RUN 1

Centrifuge Speed n rpm	Capillary Pressure z psi	Average Saturation $\overline{S}_w$
386	0.246	1.000
486	0.390	1.000
558	0.514	1.000
616	0.626	1.000
745	0.916	0.997
830	1.136	0.931
910	1.366	0.885
972	1.559	0.825
1022	1.723	0.783
1106	2.018	0.732
1240	2.536	0.661
1300	2.788	0.615
1660	4.546	0.475
20	6.731	0.430

TABLE C - 3 - 2

EXPERIMENTAL DATA

SAMPLE C, RUN 2

Centrifuge Speed n rpm	Capillary Pressure Z psi	Average Saturation $\overline{S}_w$
572	0.540	1.000
665	0.730	1.000
755	0.940	0.970
860	1.220	0.899
965	1.536	0.804
1050	1.819	0.730
1165	2.239	0.664
1260	2.619	0.616
1485	3.638	0.544
1700	4.767	0.485
1870	5.768	0.442
1980	6.467	0.421

TABLE C - 3 - 3

EXPERIMENTAL DATA

SAMPLE C, RUN 3

Centrifuge Speed n rpm	Capillary Pressure z psi	Average Saturation $\overline{S}_w$
614	0.622	1.000
775	0.991	0.984
880	1.277	0.917
1000	1.650	0.787
1100	1.996	0.727
1250	2.578	0.636
1380	3.142	0.612
1650	4.491	0.474
1830	5.524	0.447
2060	7.000	0.418

TABLE C - 4 - 1

EXPERIMENTAL DATA

SAMPLE D, RUN 1

Centrifuge Speed n rpm	Capillary Pressure Z psi	Average Saturation $\overline{S_w}$
400	0.262	1.000
600	0.589	1.000
760	0.946	1.000
910	1.356	0.960
1000	1.637	0.871
1120	2.054	0.768
1230	2.477	0.688
1340	2.940	0.646
1420	3.301	0.610
1510	3.733	0.574
1680	4.621	0.523
1810	5.364	0.494
1920	6.036	0.469
2040	6.914	0.444

TABLE C − 4 − 2

EXPERIMENTAL DATA

SAMPLE D, RUN 2

Centrifuge Speed n rpm	Capillary Pressure P_c psi	Average Saturation $\overline{S}_w$
555	0.504	1.000
690	0.780	1.000
840	1.155	1.000
1020	1.703	0.888
1165	2.222	0.794
1290	2.725	0.
1450	3.442	0. 5
1	4.621	0.54
1885	5.818	0.491
2000	6.549	0.47

TABLE C - 5 - 1

EXPERIMENTAL DATA

SAMPLE E, RUN 1

Centrifuge Speed n rpm	Capillary Pressure z psi	Average Saturation $\overline{S}_w$
400	0.176	1.000
600	0.397	1.000
700	0.540	0.905
830	0.759	0.778
960	1.016	0.666
1080	1.286	0.586
1200	1.587	0.517
1350	2.009	0.467
1450	2.317	0.431
1550	2.648	0.402
1670	3.074	0.398
1770	3.453	0.380
1860	3.843	0.354
1950	4.19?	0.342
2050	4.632	0.33?

111

TABLE C - 5 - 2

EXPERIMENTAL DATA

SAMPLE E, RUN 2

Centrifuge Speed n rpm	Capillary Pressure z psi	Average Saturation $\overline{S}_W$
400	0.176	1.000
600	0.397	1.000
670	0.495	0.930
800	0.705	0.803
900	0.893	0.730
1000	1.102	0.662
1120	1.383	0.603
1210	1.614	0.559
1350	2.039	0.507
1500	2.480	0.468
1580	2.751	0.442
1700	3.185	0.424
1800	3.691	0.414
2040	4.587	0.364

TABLE C -96 - 1

EXPERIMENTAL DATA

SAMPLE F, RUN 1

Centrifuge Speed n rpm	Capillary Pressure z psi	Average Saturation $\overline{S_w}$
400	0.239	1.000
600	0.538	1.000
670	0.671	1.000
800	0.9	1.000
900	1.211	1.000
1000	1.495	1.000
1120	1.875	0.980
1210	2.189	0.958
1360	2.765	0.893
1500	3.364	0.829
1580	3.732	0.794
1700	4.321	0.765
1830	5.007	0.739
2040	6.232	0.688

TABLE C − 6 − 2

EXPERIMENTAL DATA

SAMPLE F, RUN 2

Centrifuge Speed n rpm	Capillary Pressure z psi	Average Saturation $\overline{S_w}$
400	0.239	1.000
600	0.538	1.000
700	0.733	1.000
830	1.030	1.000
960	1.378	1.000
1080	1.744	1.000
1200	2.153	0.992
1350	2.725	0.927
1450	3.143	0.871
1550	3.592	0.815
1670	4.169	0.803
1770	4.684	0.774
1860	5.172	0.744
1950	5.685	0.725
2050	6.296	0.704

APPENDIX D

NUMERICAL RESULTS

TABLE D - 1

NUMERICAL RESULTS

SAMPLE A

Capillary Pressure % psi	Saturation $\overline{S_w}$	Saturation Approx. Method $\overline{S_w}$	(Smoothed) Num. Int. Method $\overline{S_w}$
1.096	0.982	0.986	0.986
1.151	0.990	0.979	0.979
1.308	0.952	0.955	0.954
1.397	0.942	0.939	0.939
1.651	0.880	0.892	0.892
1.651	0.911	0.892	0.892
1.872	0.855	0.852	0.852
2.145	0.783	0.805	0.805
2.240	0.787	0.790	0.790
2.559	0.745	0.742	0.742
2.642	0.726	0.731	0.731
3.328	0.655	0.650	0.650
3.543	0.634	0.629	0.629
3.889	0.598	0.599	0.599
4.121	0.593	0.582	0.582
4.494	0.558	0.556	0.556
5.113	0.525	0.522	0.521
5.378	0.499	0.509	0.509
6.054	0.495	0.481	0.481
6.769	0.443	0.458	0.458

ED - 2

NUMERICAL RESULTS

SAMPLE B

Capillary Pressure Z psi	Saturation $\overline{S_w}$	Saturation (Smoothed)	
		Approx. Method $\overline{S_w}$	Num. Int. Method $\overline{S_w}$
1.277	0.995	0.987	0.986
1.342	0.975	0.978	0.977
1.402	0.975	0.968	0.968
1.558	0.945	0.940	0.940
1.607	0.929	0.930	0.930
1.643	0.927	0.923	0.923
1.805	0.880	0.892	0.892
1.950	0.867	0.865	0.865
1.968	0.856	0.861	0.862
2.078	0.828	0.842	0.842
2.306	0.804	0.803	0.803
2.714	0.746	0.745	0.745
3.063	0.719	0.704	0.704
4.304	0.614	0.606	0.606
4.347	0.605	0.604	0.604
4.900	0.568	0.576	0.576
5.049	0.569	0.570	0.570
5.730	0.545	0.545	0.545
5.916	0.541	0.539	0.539
6.692	0.514	0.518	0.519

TABLE D - 3

NUMERICAL RESULTS

SAMPLE C

Capillary Pressure Z psi	Saturation $\overline{S_W}$	Saturation Approx. Method $\overline{S_W}$	(Smoothed) Num. Int. Method $\overline{S_W}$
0.916	0.997	0.986	0.986
0.940	0.970	0.982	0.981
0.991	0.984	0.971	0.970
1.136	0.931	0.934	0.934
1.220	0.899	0.911	0.911
1.277	0.917	0.895	0.895
1.366	0.885	0.871	0.871
1.536	0.804	0.826	0.827
1.559	0.825	0.820	0.821
1.650	0.787	0.798	0.799
1.723	0.783	0.781	0.782
1.819	0.730	0.760	0.761
1.996	0.727	0.724	0.725
2.018	0.732	0.720	0.721
2.239	0.664	0.682	0.682
2.536	0.661	0.639	0.639
2.577	0.636	0.634	0.634
2.619	0.616	0.629	0.628
2.788	0.615	0.609	0.608
3.141	0.612	0.574	0.573
3.638	0.544	0.535	0.535
4.491	0.474	0.489	0.489
4.546	0.475	0.487	0.486
4.767	0.485	0.478	0.477
5.524	0.447	0.452	0.452
5.768	0.442	0.445	0.446
6.467	0.421	0.429	0.429
6.731	0.430	0.424	0.424
7.000	0.418	0.419	0.419

TABLE D - 4

NUMERICAL RESULTS

SAMPLE D

Capillary Pressure Z psi	Saturation $\overline{S_w}$	Saturation (Smoothed) Approx. Method $\overline{S_w}$
1.703	0.888	0.890
2.222	0.794	0.789
2.725	0.709	0.710
3.442	0.625	0.629.
4.621	0.546	0.544
5.818	0.491	0.492
6.549	0.471	0.470

TABLE D - 5

NUMERICAL RESULTS

SAMPLE E

Capillary Pressure Z psi	Saturation $\overline{S_w}$	Saturation (Smoothed) Approx. Method $\overline{S_w}$
0.495	0.930	0.919
0.705	0.803	0.814
0.893	0.730	0.736
1.102	0.662	0.666
1.383	0.603	0.598
1.614	0.559	0.556
2.039	0.507	0.501
2.480	0.468	0.462
2.751	0.442	0.445
3.185	0.424	0.423
3.691	0.414	0.404
4.587	0.364	0.381

TABLE D - 6

NUMERICAL RESULTS

SAMPLE F

Capillary Pressure Z psi	Saturation $\overline{S_W}$	Saturation (Smoothed) Approx. Method $\overline{S_W}$
2.153	0.992	0.994
2.725	0.927	0.922
3.143	0.871	0.873
3.592	0.815	0.831
4.169	0.803	0.791
4.684	0.774	0.764
5.172	0.744	0.744
5.685	0.725	0.727
6.283	0.704	0.710

TABLE D – 7

MODIFIED HASSLER METHOD

SAMPLE D, RUN 2

Capillary Pressure P_c psi	Average Saturation $\overline{S_w}$	$z\overline{S_w}$	$z\overline{S_w}$ (Smoothed)	$S_w = d(z\overline{S_w})/dz$
1.703	0.888	1.513	1.522	0.464
2.222	0.794	1.764	1.745	0.401
2.725	0.709	1.932	1.934	0.352
3.442	0.625	2.152	2.168	0.305
4.621	0.546	2.523	2.510	0.287
5.818	0.491	2.857	2.862	0.300
6.549	0.471	3.084	3.083	0.304